



Article

# The Subtype Selectivity in Search of Potent Hypotensive Agents among 5,5-Dimethylhydantoin Derived $\alpha_1$ -Adrenoceptors Antagonists

Aneta Kaczor <sup>1,†</sup>, Joanna Knutelska <sup>2,†</sup>, Katarzyna Kucwaj-Brysz <sup>1</sup>, Małgorzata Zygmunt <sup>2</sup>, Ewa Żesławska <sup>3</sup>, Agata Siwek <sup>4</sup>, Marek Bednarski <sup>2</sup>, Sabina Podlewska <sup>5</sup>, Magdalena Jastrzębska-Więsek <sup>6</sup>, Wojciech Nitek <sup>7</sup>, Jacek Sapa <sup>2</sup> and Jadwiga Handzlik <sup>1,\*</sup>

- <sup>1</sup> Department of Technology and Biotechnology of Drugs, Medical College, Jagiellonian University, Medyczna 9, 30-688 Krakow, Poland; aneta.kaczor@uj.edu.pl (A.K.); katarzyna.kucwaj@uj.edu.pl (K.K.-B.)
  - <sup>2</sup> Department of Pharmacodynamics, Medical College, Jagiellonian University, Medyczna 9, 30-688 Krakow, Poland; joanna.1.knutelska@uj.edu.pl (J.K.); malgorzata.zygmunt@uj.edu.pl (M.Z.); marek.bednarski@uj.edu.pl (M.B.); jacek.sapa@uj.edu.pl (J.S.)
  - <sup>3</sup> Institute of Biology and Earth Sciences, University of the National Education Commission, Podchorążych 2, 30-084 Krakow, Poland; ewa.zeslawska@up.krakow.pl
  - <sup>4</sup> Department of Pharmacobiology, Medical College, Jagiellonian University, Medyczna 9, 30-688 Krakow, Poland; agat.siwiek@uj.edu.pl
  - <sup>5</sup> Maj Institute of Pharmacology, Polish Academy of Sciences, Department of Medicinal Chemistry, Smętna 12, 31-343 Krakow, Poland; smusz@if-pan.krakow
  - <sup>6</sup> Department of Clinical Pharmacy, Medical College, Jagiellonian University, Medyczna 9, 30-688 Krakow, Poland; m.jastrzebska-wiesek@uj.edu.pl
  - <sup>7</sup> Faculty of Chemistry, Jagiellonian University, Gronostajowa 2, 30-387 Krakow, Poland; wojciech.nitek@uj.edu.pl
- \* Correspondence: j.handzlik@uj.edu.pl; Tel.: +48-12-620-55-80
- <sup>†</sup> These authors contributed equally to this work.



**Citation:** Kaczor, A.; Knutelska, J.; Kucwaj-Brysz, K.; Zygmunt, M.; Żesławska, E.; Siwek, A.; Bednarski, M.; Podlewska, S.; Jastrzębska-Więsek, M.; Nitek, W.; et al. The Subtype Selectivity in Search of Potent Hypotensive Agents among 5,5-Dimethylhydantoin Derived  $\alpha_1$ -Adrenoceptors Antagonists. *Int. J. Mol. Sci.* **2023**, *24*, 16609. <https://doi.org/10.3390/ijms242316609>

Academic Editor: Stefan Cristian Vesa

Received: 28 October 2023

Revised: 18 November 2023

Accepted: 19 November 2023

Published: 22 November 2023



**Copyright:** © 2023 by the authors. Licensee MDPI, Basel, Switzerland. This article is an open access article distributed under the terms and conditions of the Creative Commons Attribution (CC BY) license (<https://creativecommons.org/licenses/by/4.0/>).

**Abstract:** In order to find new hypotensive drugs possessing higher activity and better selectivity, a new series of fifteen 5,5-dimethylhydantoin derivatives (1–15) was designed. Three-step syntheses, consisting of N-alkylations using standard procedures as well as microwaves, were carried out. Compounds 7–9 had crystallographic structure determined. All of the synthesized 5,5-dimethylhydantoin derivatives were tested for their affinity to  $\alpha_1$ -adrenergic receptors ( $\alpha_1$ -AR) using both in vitro and in silico methods. Most of them displayed higher affinity ( $K_i < 127.9$  nM) to  $\alpha_1$ -adrenoceptor than urapidil in radioligand binding assay. Docking to two subtypes of adrenergic receptors,  $\alpha_{1A}$  and  $\alpha_{1B}$ , was conducted. Selected compounds were tested for their activity towards two  $\alpha_1$ -AR subtypes. All of them showed intrinsic antagonistic activity. Moreover, for two compounds (1 and 5), which possess o-methoxyphenylpiperazine fragments, strong activity ( $IC_{50} < 100$  nM) was observed. Some representatives (3 and 5), which contain alkyl linker, proved selectivity towards  $\alpha_{1A}$ -AR, while two compounds with 2-hydroxypropyl linker (11 and 13) to  $\alpha_{1B}$ -AR. Finally, hypotensive activity was examined in rats. The most active compound (5) proved not only a lower effective dose than urapidil but also a stronger effect than prazosin.

**Keywords:**  $\alpha_1$ -adrenoceptor; 5,5-dimethylhydantoin; crystallography; molecular modelling;  $\alpha_{1A}$ ;  $\alpha_{1B}$

## 1. Introduction

The  $\alpha_1$ -adrenoceptors ( $\alpha_1$ -ARs) belong to the G protein-coupled receptor (GPCR) and play a fundamental role in the physiology of the sympathetic nervous system [1]. They are activated by the endogenous catecholamines, norepinephrine and epinephrine and mediate various physiological effects, such as vascular and urogenital smooth muscle contraction [2]. Pharmacologically,  $\alpha_1$ -ARs are an important cellular target for the treatment of several pathologies [3], e.g., hypertension [4–6], benign prostatic hyperplasia (BPH) [7], and lower urinary tract symptoms (LUTS) [8,9]. Nowadays, three subtypes of  $\alpha_1$ -adrenoceptors,

namely  $\alpha_{1A}$ ,  $\alpha_{1B}$ , and  $\alpha_{1D}$ , have been identified based on molecular cloning techniques and pharmacological studies [1]. All three  $\alpha_1$ -AR subtypes are present in blood vessels [10], whereas the  $\alpha_{1B}$  subtype contributes to vasoconstriction and blood pressure control in humans [11–13]. Interestingly, the expression of vascular  $\alpha_1$ -AR subtypes changes with age. In the mammary artery,  $\alpha_{1B}$ -AR expression increases 2-fold in patients aged 65 years or older compared to patients younger than 55 years. Consequently, the  $\alpha_{1B}$ -AR is the predominant subtype in the arteries in older patients ( $\geq 65$  years) [10]. Data from human studies indicate that  $\alpha_{1B}$ -AR predominates in epicardial coronary artery endothelial cells (90–95% of total  $\alpha_1$ -AR mRNA) [14]. Recently, a molecular study confirmed a statistically significant increase in the expression of  $\alpha_{1B}$ -AR in human peripheral mononuclear cells from hypertension patients. The increase in  $\alpha_{1B}$ -AR mRNA levels correlates with the increase in systolic blood pressure and plasmatic homocysteine levels [15]. Thus,  $\alpha_1$ -AR antagonists are attractive therapeutic targets for the treatment of hypertension. Blockade of  $\alpha_1$ -ARs reduces vascular resistance and venous capacitance [16], consequently decreasing peripheral resistance and lowering blood pressure [6]. It is also well established that  $\alpha_1$ -adrenoceptor antagonists have beneficial effects on lipids profile and glucose metabolism [17–27]. Recent clinical studies have shown that therapy with  $\alpha_1$ -AR blockers is associated with a lower rate of readmission for heart failure and mortality [28].

The  $\alpha_{1A}$ - and  $\alpha_{1B}$ -ARs are present in the human myocardium and do not appear to have an important role in the regulation of heart function under normal physiological conditions but increase importance under pathological conditions [29]. During cardiac ischemia and post-ischemic reperfusion,  $\alpha_1$ -adrenergic stimulation may play a significant role in the generation of arrhythmias because myocardial ischemia causes an increase in  $\alpha_1$ -ARs density and intracellular  $Ca^{2+}$  overload [30–34]. The increase in intracellular  $Ca^{2+}$  signaling, in response to  $\alpha_1$ -adrenergic stimulation, is mediated by the  $\alpha_{1A}$ -AR [35]. Data from animal studies demonstrate that the  $\alpha_{1A}$ -AR antagonists have antiarrhythmic effects [36]. Therefore, this subtype is an interesting target for the treatment of arrhythmias.

In this context, the search for antagonists of  $\alpha_1$ -ARs is an important issue in the discovery and development of new therapeutic agents. Prazosin, which was the first marketed antihypertensive drug with  $\alpha$ -adrenolytic activity and two further pharmaceuticals in this class, terazosin and doxazosin [4,37,38], contain a piperazine-1,4-diyl moiety (Figure 1) [39,40]. Pharmacological studies of  $\alpha_1$ -ARs antagonists demonstrated that an *o*-methoxyphenylpiperazine moiety plays a significant role in the affinity to this subtype [39–42], and this structural fragment is also a part of structures of urapidil and naftopidil (Figure 1) [39]. Urapidil, a well-known antihypertensive drug, acts as an  $\alpha_1$ -AR antagonist and 5-HT<sub>1A</sub> agonist [43], while naftopidil is an  $\alpha_1$ -AR blocker with 3-fold higher affinity for  $\alpha_{1D}$ - than for  $\alpha_{1A}$ -AR subtype, and is commonly used in the treatment of patients with LUTS/BPH [44].

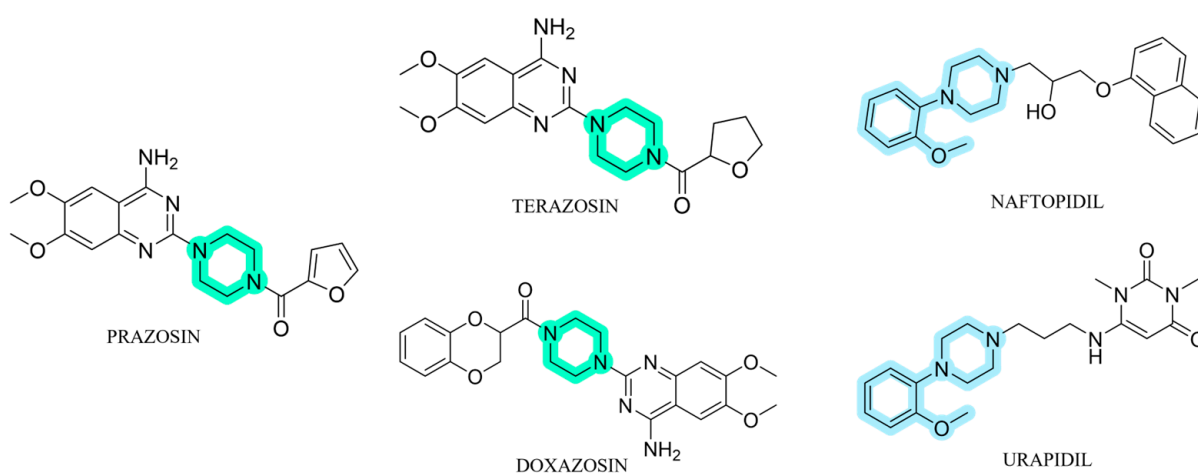


**Figure 1.** The structures of already approved  $\alpha_1$ -adrenoceptors ( $\alpha_1$ -ARs) antagonists.

Our previous studies described syntheses and pharmacological properties of phenylpiperazine derivatives of phenytoin that displayed *in vitro* high affinity for  $\alpha_1$ -ARs and antagonistic properties in functional bioassays (Figure 2) [45–47]. Several compounds also showed antiarrhythmic effects via an  $\alpha_1$ -ARs dependent antagonistic action [41]. In addition, the derivative with *o*-methoxyphenylpiperazine moiety displayed hypotensive activity in an animal model [41]. The already described modifications included different types of substituents on piperazine, modification on linker (length and/or branching with hydroxy group) and modification on nitrogen atom N3 of hydantoin—ester or aliphatic chain (Figure 2). Nevertheless, we succeeded with the synthesis of compounds with better *in vitro* activity than reference AZ-99. Those compounds are characterized by high hydrophobic properties and moderate solubility. The continuation of this work led to the synthesis of compound PI, which was the first derivative without two aromatic rings in position 5 of hydantoin (two methyl groups instead) and with a benzyl group in position N3 (Figure 2) [48]. Based on structure-activity relationship (SAR) analysis from previous results and choosing compound PI as the lead structure, we designed the novel series of compounds (1–15, Table 1). In order to keep the balance between appropriate hydrophobicity and still meet the criteria of Barbaro’s pharmacophore model for  $\alpha_1$ -ARs activity [49], two chlorine atoms were introduced to the benzyl group (Figure 2). Moreover, the lead optimization concerned substituents on piperazine and linker type—length/(un)branching with the hydroxy group. Hence, the main goal of the present study was to investigate the impact of performed modifications on *in vitro* affinity for  $\alpha_1$ -ARs, as well as intrinsic activity at the  $\alpha_{1A}$  and  $\alpha_{1B}$  subtypes. Additionally, selected derivatives were investigated *in vivo* to determine an influence on arterial blood pressure in rats. The structural studies were enriched by X-ray crystallography and molecular docking to  $\alpha_1$ -ARs subtypes.

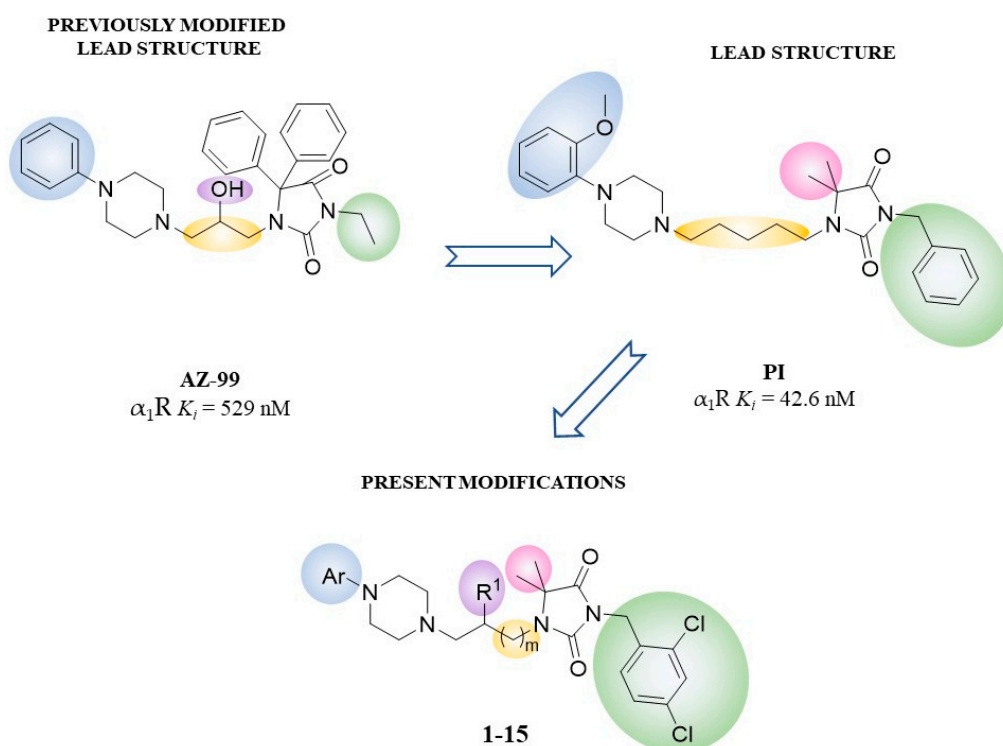


**Figure 2.** Structures of previously reported lead structure (AZ-99), the lead structure for the present study (PI), as well as the area of herein investigated structural modifications.

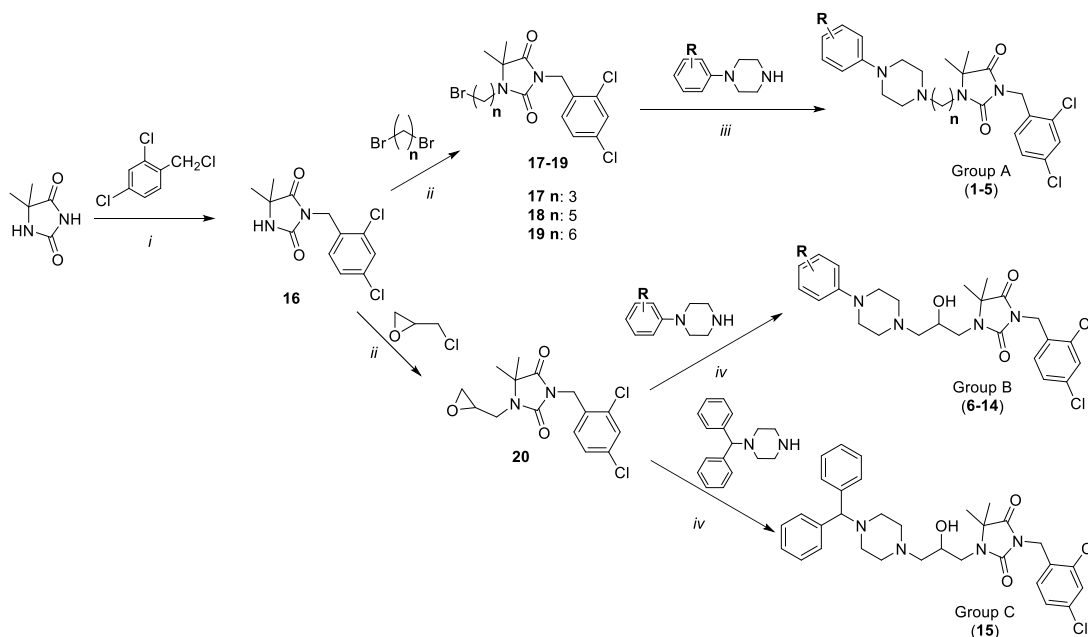
**Table 1.** Structures of obtained 5,5-dimethylhydantoin derivatives (1–15).

Cpd	Group	n	R	Cpd	Group	n	R
1	A	3	2-MeO	9	B	-	2,4-diF
2	A	3	2,3-diCl	10	B	-	3,4-diCl
3	A	5	H	11	B	-	2-CN
4	A	6	3,4-diCl	12	B	-	3,4-diMe
5	A	6	2-MeO	13	B	-	2-MeO
6	B	-	H	14	B	-	3-MeO
7	B	-	2-F	15	C	-	-
8	B	-	4-F				

## 2. Results

### 2.1. Chemistry

Syntheses of compounds 1–15 (Table 1) were performed according to Scheme 1.



**Scheme 1.** Syntheses of compounds 1–15; (i)  $K_2CO_3$ , TEBA, acetone, reflux, 4 h; (ii)  $K_2CO_3$ , TEBA, acetone, rt, 120–168 h; (iii)  $K_2CO_3$ , acetone, reflux, 4–11 h; (iv)  $\mu w$ , 300–450 W, 3–7 min.

Syntheses of compounds 7–9, 15, 16 and 18–20 were published before [48,50]. Syntheses of obtained compounds consisted of (i) N3-alkylation, (ii) N1-alkylation, and (iii or iv) arylpiperazine N-alkylation with suitable alkylation agents (17–20). Firstly, 5,5-dimethylhydantoin was reacted with 2,4-dichlorobenzyl chloride to obtain intermediate 16 (i, Scheme 1). In the next reaction (ii), N1-alkylation was conducted using dibromoalkyl (17–19, Group A) or 2-(chloromethyl)oxirane (20, Group B and C). The final N-alkylation was carried out using 1-phenylpiperazine derivatives to obtain products from Group A (1–5, Scheme 1) and Group B (6–14, Scheme 1). However, conditions for those two groups were different. In Group A, the reaction was carried out using acetone and potassium carbonate,

while for Group B, the reaction was conducted using microwave ( $\mu\text{w}$ ) irradiation. In the case of compound **15** (Group C), intermediate **20** was reacted with 1-benzhydrylpiperazine under microwave conditions.

## 2.2. X-ray Crystallographic Studies

The molecular geometry in the crystals of **7**, **8**, and **9** with the atom numbering schemes is shown in Figure 3.

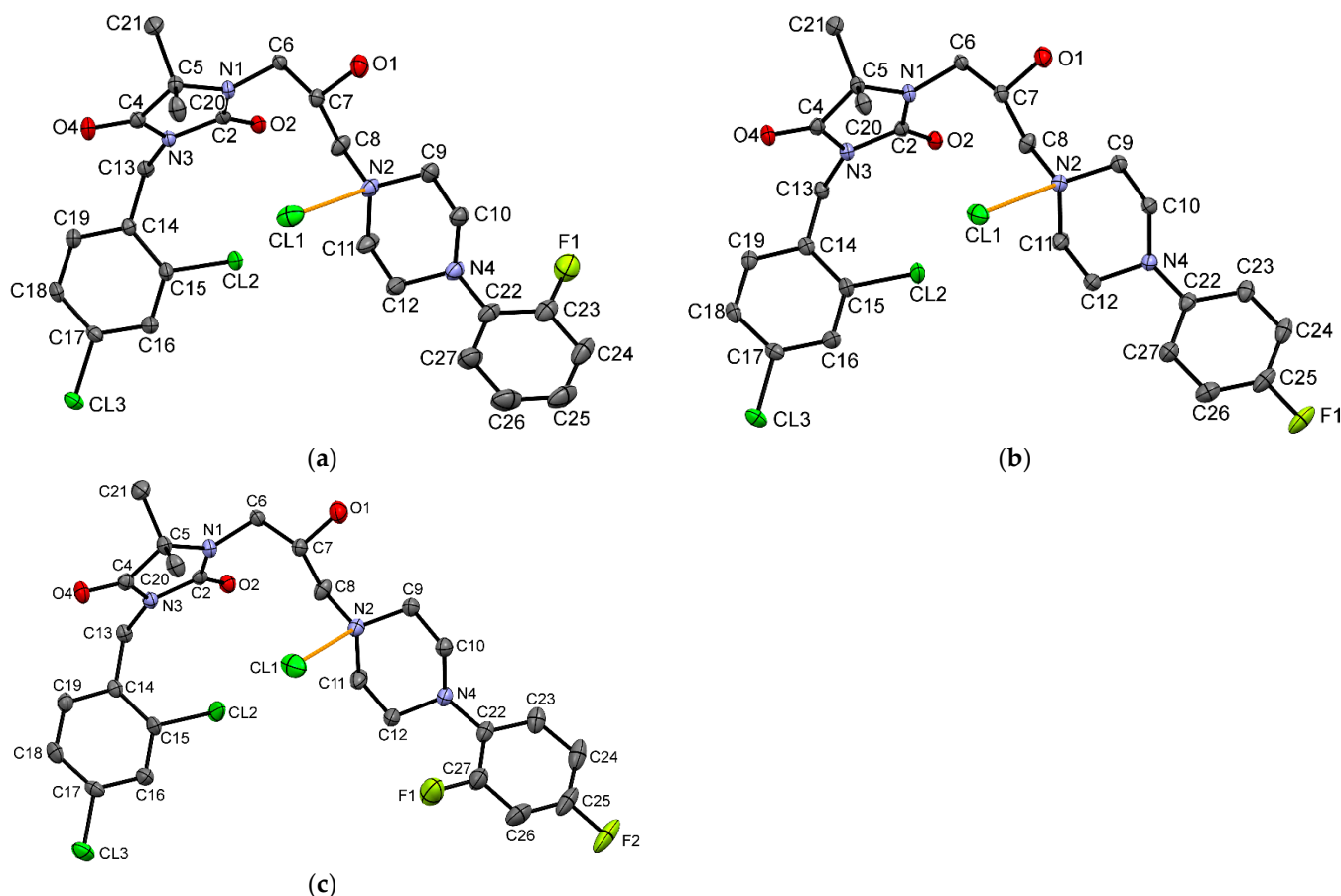


**Figure 3.** The molecular geometry of (a) **7**, (b) **8** and (c) **9**, with the atom numbering schemes. Hydrogen atoms have been omitted for clarity. Displacement ellipsoids are drawn at the 50% probability level. Orange lines show hydrogen bonds between the chloride anion and the protonated N2 atom.

The overall shape of these three molecules is very similar (Figure 4). The linker, having a bent conformation, consists of three methylene units with a hydroxy group located at the second carbon atom. The oxygen atom of the hydroxy group is engaged in the intramolecular C9-H9...O1 hydrogen bond. Furthermore, the geometry of the linker is stabilized by intermolecular interactions, in which O-H...Cl and C-H...O hydrogen bonds are involved. Similar geometry was observed in another hydantoin derivative with the same linker [49].

Small differences are visible in the mutual orientation of hydantoin and aromatic rings, as well as hydantoin and piperazine rings. The piperazine ring adopts chair conformation with an equatorial position of substituents at N2 and N4 atoms. The investigated compounds have different substituents at the aromatic ring, which is connected to the piperazine ring, namely 2-F for **7**, 4-F for **8** and 2,4-di-F for **9**. The angle between the planes of the aromatic ring at the N4 atom and the carbon atoms of the piperazine ring is 49.86, 41.99 and 53.82° for **7**, **8** and **9**, respectively. The values of this angle for **7**, **8** are higher

than in other crystal structures containing 4-(2-fluorobenzene)piperazine (the range of this angle 35.75–46.28°) or 4-(4-fluorobenzene)piperazine moiety (the range of this angle 11.52–35.68°) deposited in Cambridge Structure Database (CSD) [51]. There is no deposited crystal structure containing 4-(2,4-difluorobenzene)piperazine moiety in the CSD, which is present in **9**. The introduction of the second fluorine atom into the aromatic ring increases the value of this interplanar angle. The biggest difference in the geometry of analyzed molecules is observed in the location of 2-fluoro substituent of **7** in comparison to 2-fluoro substituent of **9**; namely, these substituents are on opposite sides (Figure 4).

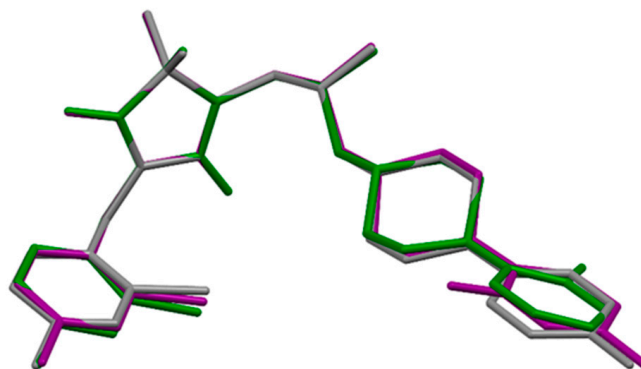


**Figure 4.** The overlap of the hydantoin rings of **7** (green), **8** (grey) and **9** (purple).

In the presented crystal structures, the chlorine anion is involved in a charge-assisted hydrogen bond with a protonated N2 atom (Figure 3). The intermolecular interactions in the crystals are dominated by N-H...Cl, O-H...Cl, C-H...Cl and C-H...O hydrogen bonds. Additionally, C-H...F contacts are observed for structures containing 4-F substituent.

### 2.3. Affinity for $\alpha_1$ -Adrenoceptors

In the first step, all synthesized compounds (**1–15**) were tested in vitro for their affinity for  $\alpha_1$ -ARs on rat cerebral cortex by the radioligand binding assay using [<sup>3</sup>H]-prazosin as a specific radioligand. The affinity described by  $K_i$  (nM) values are given in Table 2. A majority of compounds (**1**, **3**, **5–9**, **11**, **13**) presented high affinity for  $\alpha_1$ -ARs ( $K_i \leq 100$  nM). These compounds were identified to be more potent than urapidil, but none was as potent as the reference antagonist (prazosin). Among the novel compounds, four derivatives (**2**, **4**, **12**, **14**) showed moderate affinity to  $\alpha_1$ -ARs ( $100 < K_i \leq 535$  nM). The newly synthesized derivatives, excluding compounds **2**, **10**, and **15**, presented higher affinity for the  $\alpha_1$ -ARs, when compared to compound **AZ-99**.

**Table 2.**  $\alpha_1$ -adrenoceptor affinity ( $K_i$ ) for the tested compounds (**1–15**) and references (**AZ-99**, prazosin, and urapidil) [39,45].

Compound	$K_i$ (nM)
<b>1</b>	31.0
<b>2</b>	535.0
<b>3</b>	43.0
<b>4</b>	255.0
<b>5</b>	12.7
<b>6</b>	53.0
<b>7</b>	100.0
<b>8</b>	44.0
<b>9</b>	42.0
<b>10</b>	778.0
<b>11</b>	26.0
<b>12</b>	270.0
<b>13</b>	29.0
<b>14</b>	289.0

**Table 2.** *Cont.*

Compound	$K_i$ (nM)
<b>15</b>	2443.0
<b>AZ-99</b>	529.0 <sup>a</sup>
<b>Prazosin</b>	0.24 <sup>a</sup>
<b>Urapidil</b>	127.9 <sup>b</sup>

Inhibition constants ( $K_i$ ) values were obtained from three independent experiments in duplicates. <sup>a</sup> Results were published previously [45]; <sup>b</sup> Result was published previously [39].

#### 2.4. Intrinsic Activity

In the next step, selected compounds (**1–3**, **5–9**, **11–14**) were tested in vitro for their antagonistic activity at the  $\alpha_1$ -AR subtypes using the cells expressing mitochondrially-targeted aequorin and one of the human adrenergic receptors  $\alpha_{1A}$  or  $\alpha_{1B}$ . The intrinsic activity expressed as  $IC_{50}$  values is presented in Table 3. The subtype selectivity for  $\alpha_{1A}$  and  $\alpha_{1B}$  was calculated as  $IC_{50(\alpha_{1B-AR})}/IC_{50(\alpha_{1A-AR})}$  and  $IC_{50(\alpha_{1A-AR})}/IC_{50(\alpha_{1B-AR})}$  ratio, respectively.

**Table 3.** Intrinsic activity at the  $\alpha_1$ -ARs ( $\alpha_{1A}$ ,  $\alpha_{1B}$ ) for tested compounds and references.

Compound	$\alpha_{1A}$ -AR		$\alpha_{1B}$ -AR		Selectivity Ratio	
	$IC_{50}$ <sup>a</sup> (nM)	Profile	$IC_{50}$ <sup>a</sup> (nM)	Profile	$\alpha_{1A}/\alpha_{1B}$ <sup>b</sup>	$\alpha_{1B}/\alpha_{1A}$ <sup>c</sup>
<b>1</b>	90.62	Antagonist	10.71	Antagonist	8.46	0.12
<b>2</b>	1730.00	Antagonist	1146.00	Antagonist	1.51	0.66
<b>3</b>	290.00	Antagonist	3.27	Antagonist	88.73	0.01
<b>5</b>	0.02	Antagonist	0.002	Antagonist	10.00	0.10
<b>6</b>	5909.00	Antagonist	905.00	Antagonist	6.53	0.15
<b>7</b>	1415.00	Antagonist	483.90	Antagonist	2.92	0.34
<b>8</b>	816.70	Antagonist	170.40	Antagonist	4.79	0.21
<b>9</b>	162.40	Antagonist	147.40	Antagonist	1.10	0.91
<b>11</b>	162.30	Antagonist	359.10	Antagonist	0.45	2.21
<b>12</b>	3136.00	Antagonist	377.30	Antagonist	8.31	0.12
<b>13</b>	138.70	Antagonist	331.10	Antagonist	0.42	2.39
<b>14</b>	1221.00	Antagonist	1366.00	Antagonist	0.89	1.12
<b>Tamsulosin</b>	0.03	Antagonist	0.48	Antagonist	0.06	16.00
<b>Terazosin</b>	4.52	Antagonist	0.67	Antagonist	6.70	0.15
<b>Prazosin</b>	0.72	Antagonist	0.17	Antagonist	4.25	0.24
<b>Phenylephrine</b>	23.64	Agonist	2.31	Agonist	10.25	0.10

<sup>a</sup>  $IC_{50}$  values are means of three independent experiments in duplicates; <sup>b</sup> selectivity for  $\alpha_{1B}$ -AR ( $IC_{50(\alpha_{1A-AR})}/IC_{50(\alpha_{1B-AR})}$ ); <sup>c</sup> selectivity for  $\alpha_{1A}$ -AR ( $IC_{50(\alpha_{1B-AR})}/IC_{50(\alpha_{1A-AR})}$ ).

All tested compounds demonstrated antagonistic activity at the  $\alpha_1$ -AR subtypes. The strong ( $IC_{50} < 100$  nM) or moderate ( $100$  nM  $< IC_{50} < 200$  nM)  $\alpha_{1A}$ -AR antagonistic intrinsic activity was observed for compounds **1** and **5**, or **9**, **11**, and **13**, respectively. Compound **5** was more potent at the  $\alpha_{1A}$ -AR than terazosin and prazosin and generally similar when compared to tamsulosin (Figure 5a). The strong  $\alpha_{1B}$ -AR antagonistic intrinsic activity ( $IC_{50} < 11$  nM) was identified for compounds **1**, **3**, and **5**. Interestingly, compound **5** was more potent at the  $\alpha_{1B}$ -AR than all reference drugs: prazosin, terazosin and tamsulosin (Figure 5b). This compound was found to be the most potent  $\alpha_1$ -AR antagonist in the present group of derivatives of 5,5-dimethylhydantoin. In terms of subtype selectivity, compounds **5** and **3** displayed moderate (10-fold) and much higher (~90-fold) selectivity for  $\alpha_{1B}$ -AR over  $\alpha_{1A}$ -AR, respectively. Compounds **11** and **13** demonstrated slightly higher (~2-fold) selectivity for  $\alpha_{1A}$ -AR over  $\alpha_{1B}$ -AR. The reference drugs, prazosin and terazosin, did not show subtype selectivity, while tamsulosin demonstrated moderate selectivity for  $\alpha_{1A}$ -AR (over  $\alpha_{1B}$ -AR), according to the literature data [52,53].

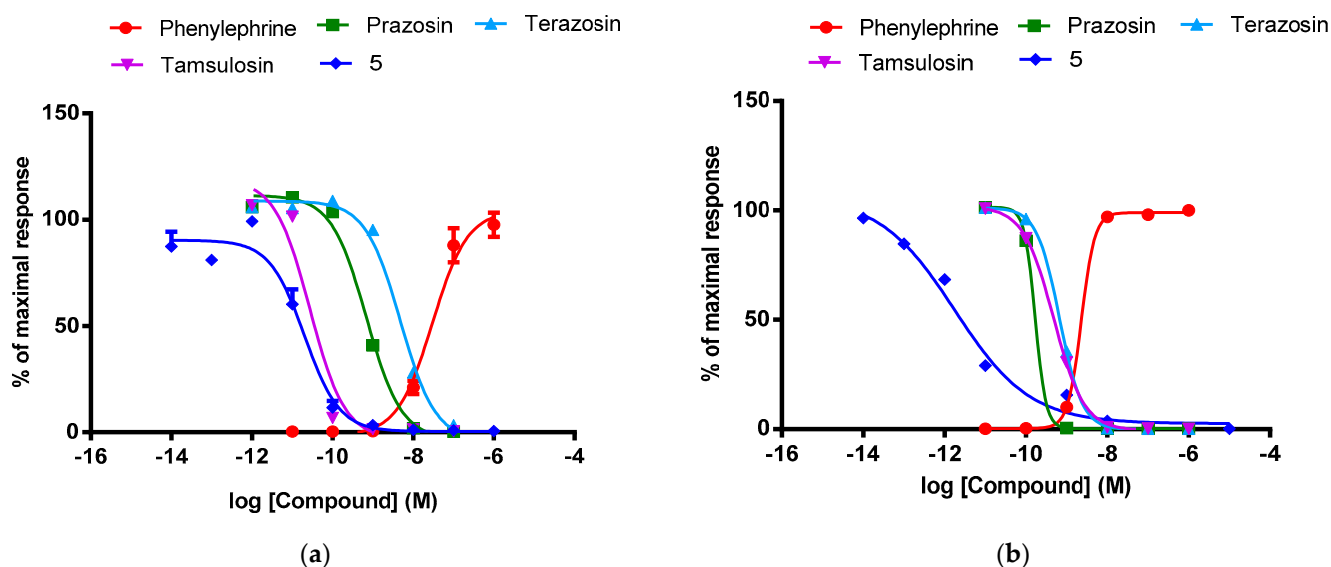


**Figure 5.** Concentration-response curves of phenylephrine, prazosin, terazosin, tamsulosin and compound 5 at the adrenergic (a)  $\alpha_{1A}$  and (b)  $\alpha_{1B}$  receptors. The values (%) are expressed as a percentage of the action of the reference agonist phenylephrine at the dose of  $EC_{80}$  (100%).

### 2.5. Molecular Modelling

The compounds were docked to the inactive-state models of adrenergic receptors  $\alpha_{1A}$  and  $\alpha_{1B}$ , constructed on the basis of the GPCRdb data. The ligand-protein contacts occurring in the obtained complexes are present in the form of the interaction matrices with  $\alpha_{1A}$  (Figure 6) and  $\alpha_{1B}$  receptors (Figure 7).

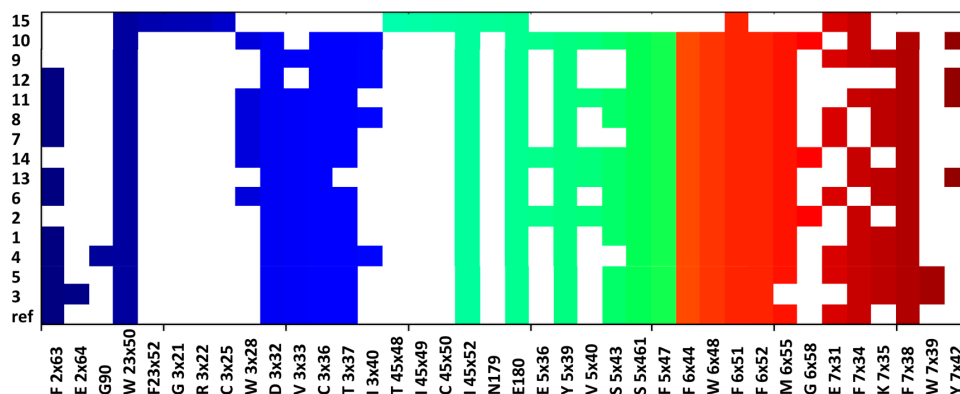


**Figure 6.** Ligand-protein interactions present in the compound complexes with  $\alpha_{1A}$  receptors.

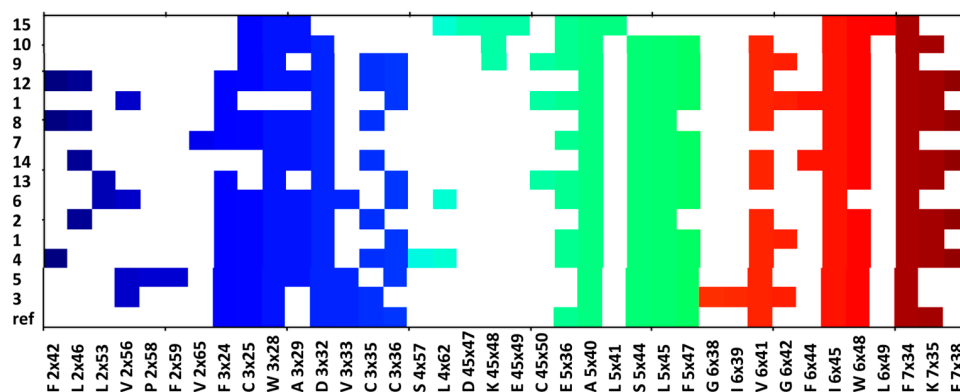


**Figure 7.** Ligand-protein interactions present in the compound complexes with  $\alpha_{1B}$  receptors.

The contact patterns presented in both Figures 6 and 7 show that the compounds consistently interact with the aspartic acid from the third transmembrane helix (TM3), D 3 × 32, for both  $\alpha_{1A}$  and  $\alpha_{1B}$  receptor subtype; the respective interaction is not present only for **15** (it is missing for both  $\alpha_{1A}$  and  $\alpha_{1B}$ ), which was characterized by the lowest affinity to  $\alpha_1$  receptor ( $K_i = 2443$  nM).

In addition, all the compounds make contact with two residues from the second extracellular loop (ECL2): I 45 × 52, E180, and also with F × 51 when  $\alpha_{1A}$  is taken into account and with A 5 × 40, I 6 × 45, and F 7 × 34, when  $\alpha_{1B}$  is considered.

In general, the interaction matrices show that the compounds adopted similar poses in the receptor binding sites: they consistently interact with the same set of residues from TM3, TM5, TM6, and TM7.

The comparison of **13** (significantly better binder of  $\alpha_{1A}$ ) position in  $\alpha_{1A}$  and  $\alpha_{1B}$  (Figure 8) revealed that although the position of piperazine is similar for both receptor subtypes, the hydrogen bond with D 3 × 32 is formed only with  $\alpha_{1A}$ . Although compound **13** makes contact with D 3 × 32, the protonated nitrogen from the piperazine moiety is too far from the oxygen from the aspartic acid to make contact via a strong hydrogen bond. In addition, the methoxy moiety points towards TM5 for  $\alpha_{1A}$ , whereas in **13**- $\alpha_{1B}$  complex it is oriented with the closest proximity to TM6.

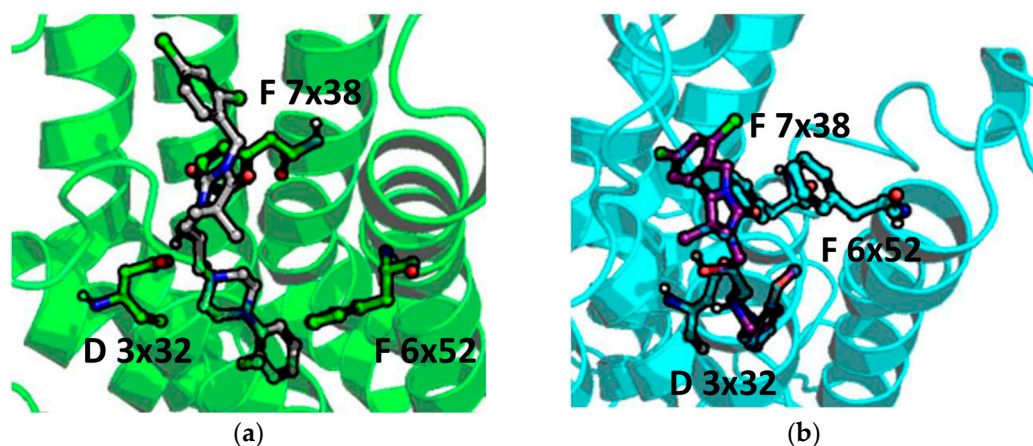


**Figure 8.** Docking results of **13** to (a)  $\alpha_{1A}$  and (b)  $\alpha_{1B}$ .

Examining the ligand-protein interactions occurring for **PI** and **3** (Figure 9), it appears that the compound orientation in the binding site of both  $\alpha_{1A}$  and  $\alpha_{1B}$  is similar, and the piperazine moieties (forming the strongest interaction with the receptor) are almost aligned in both cases, which can explain the similar activity profile of **PI** and compound **3**. The introduction of di-Cl into the benzyl ring did not influence the overall compound pose but resulted in the formation of the additional interactions with W 7 × 39 in the case of  $\alpha_{1A}$ , and V 2 × 56 for  $\alpha_{1B}$ . However, as the di-Cl substitution faces towards extracellular part of the receptor, it probably does not influence compound affinity to such an extent, and the contact pattern of non-substituted **PI** is strong enough to provide the strong compound binding.

The low affinity of **15** is also reflected in docking studies, in which it adopted a flipped position in comparison to all remaining compounds for both  $\alpha_{1A}$  and  $\alpha_{1B}$  (Figure 10). As a result, the piperazine in **15** is located too far from the D 3 × 32 residue, and the hydrogen bond between the protonated nitrogen of piperazine and aspartic acid from TM3 cannot be formed. Instead, the piperazine interacts with E180 from ECL2 for  $\alpha_{1A}$ , and K 45 × 48, E 45 × 49, C 45 × 50 for  $\alpha_{1B}$ ; however, the overall position of **15** in the receptor binding site (for both  $\alpha_{1A}$ , and  $\alpha_{1B}$ ) is very shallow (especially for  $\alpha_{1A}$ ) and does not provide sufficient contact network to strongly fit the compound in the binding pocket.

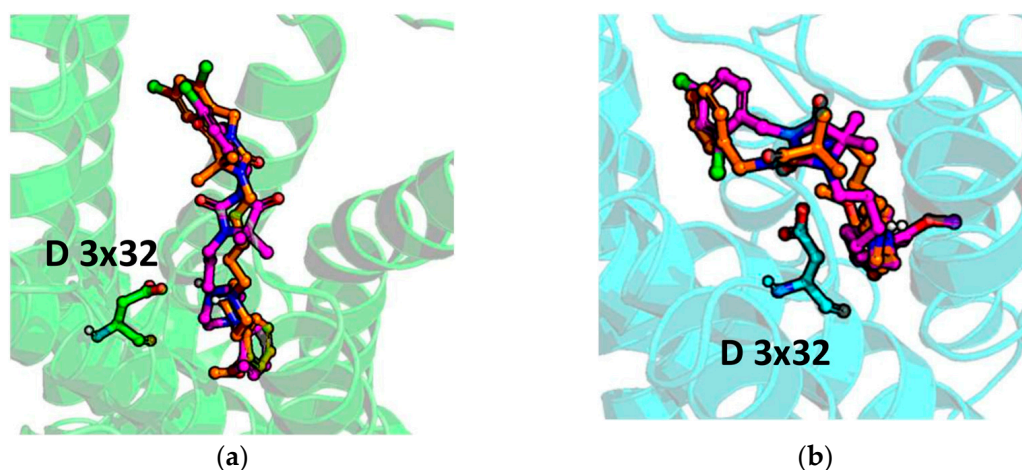


**Figure 9.** Docking results of PI (orange) and 3 (magenta) to (a)  $\alpha_{1A}$  and (b)  $\alpha_{1B}$ .

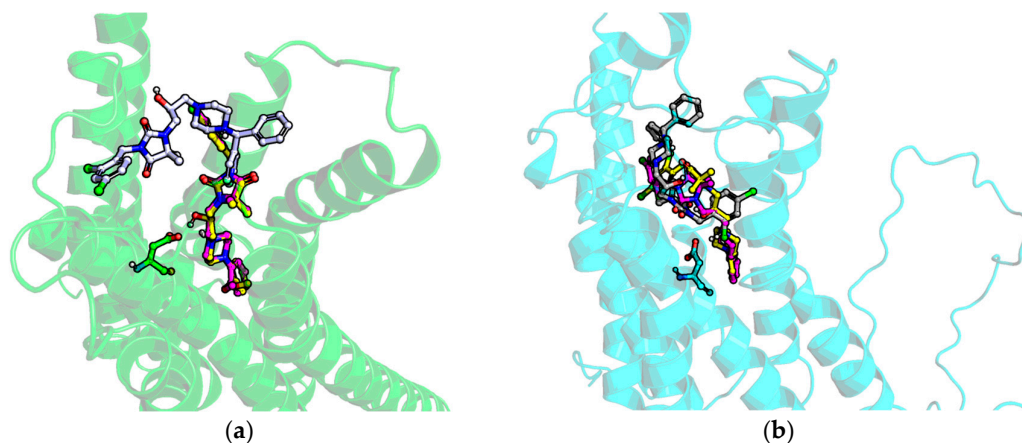


**Figure 10.** Docking results of 15 (grey), 13 (yellow), and 3 (magenta) to (a)  $\alpha_{1A}$  and (b)  $\alpha_{1B}$ .

### 2.6. The Influence on Blood Pressure in Rats

In the next step, the hypotensive activity of novel compounds 1–3, 5–9, and 11–14 was determined after i.v. administration to normotensive anesthetized rats. All results are shown in Supplementary Table S1. Four compounds (1, 3, 5, 13) proved statistically significant reduction of systolic and diastolic blood pressure. For these compounds, the hypotensive activity expressed as a percentage of decreased systolic and diastolic blood pressure is displayed in Figures 11a and 11b, respectively.

Compound 5 administered at the dose 0.0625 mg/kg, significantly reduced systolic blood pressure by 13.1–10.6% and diastolic blood pressure by 14.8–10.5% from the fifth minute of the observation period. Compound 13 at the dose 2.0 mg/kg, significantly decreased systolic blood pressure by 23.2–10.8% and diastolic blood pressure by 37.6–13.0% from the fifth minute after administration. Compound 3 at the dose 2.0 mg/kg, significantly reduced systolic blood pressure by 13.7–9.0% and diastolic blood pressure by 14.6–12.3% from the tenth minute after administration. Compound 1 at the dose 2.0 mg/kg, significantly reduced systolic blood pressure by 14.3–11.2% and diastolic blood pressure by 14.9–13.2% from the tenth minute of the observation period. Urapidil (used as a reference compound) at the lowest hypotensive dose (1.0 mg/kg) significantly decreased systolic blood pressure by 16.8–13.1% and diastolic blood pressure by 20.9–15.7% from the fifth minute after administration.

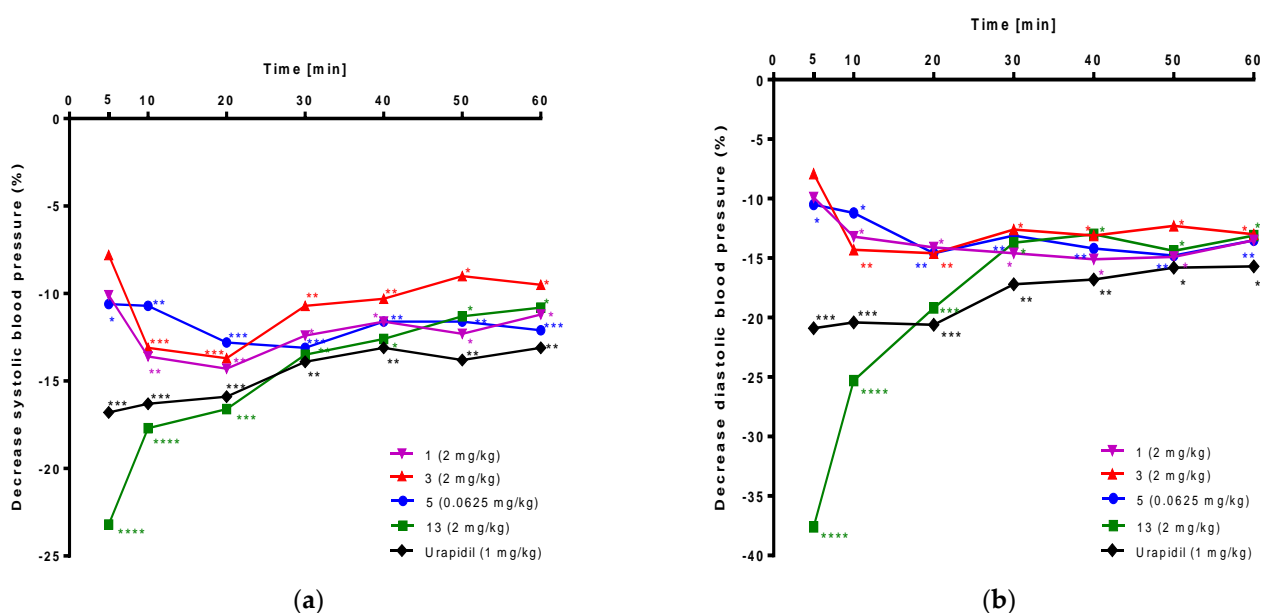


**Figure 11.** Hypotensive activity of **1**, **3**, **5**, **13**, and urapidil tested after i.v. administration to anesthetized normotensive rats. Results are expressed as a percentage of decrease (a) systolic and (b) diastolic blood pressure. Statistical analysis: two-way ANOVA and Sidak's multiple comparisons test. Statistically significant: \*  $p < 0.05$ , \*\*  $p < 0.02$ , \*\*\*  $p < 0.01$ , \*\*\*\*  $p < 0.001$ , vs. control group (vehicle treatment);  $n = 6$  rats per each group.

### 3. Discussion

The new group of 5,5-dimethylhydantoin derivatives (**1**–**15**) is characterized by modifications in two fragments: arylpiperazine and alkyl linker (Figure 2). The first one involves un-, mono- and disubstituted phenyl ring (Group A and B, Table 1) or diphenylmethyl moiety (Group C, Table 1). The other embraced either three different lengths of chain ( $n = 3, 5$  or  $6$ , Group A) or branching with hydroxyl group (Group B and C). The current design was based on a previously found active compound, **PI** (Figure 2), and accordingly, final products possess 5,5-dimethyl- fragment. Furthermore, the benzyl moiety connected to N3 position of hydantoin was slightly modified by the addition of two chlorine atoms to achieve proper hydrophobic properties. Taking into consideration previously obtained active compounds, described modifications of moieties attached to N1 position enabled to carry out structure–activity relationship (SAR) analysis of obtained compounds with potential influence on  $\alpha_1$ -ARs.

Affinity values for  $\alpha_1$ -ARs were determined for all compounds (**1**–**15**) using the radioligand binding assay. Nine compounds (**1**, **3**, **5**–**9**, **11**, and **13**) displayed  $K_i$  lower than urapidil (Table 2). Among the four, the most potent compounds (**1**, **3**, **5**, **13**) proved to have high affinity for  $\alpha_1$ -ARs ( $K_i = 31.0, 43.0, 12.7, 29.0$  nM, respectively), three ones (**1**, **5**, **13**) contain an *o*-methoxyphenylpiperazine fragment in their structure. Moreover, compound **11**, possessing a cyano group at the *o*-position of the phenyl ring, also showed a high affinity for these receptors ( $K_i = 26.0$  nM). Nevertheless, the most potent compound (**5**) possesses an *o*-methoxyphenylpiperazine fragment and hexyl linker at the N1-position of hydantoin. Moreover, current studies results proved that presence of chlorine in phenyl ring is not advantageous (**1** vs. **2**, **5** vs. **4**, and **6** vs. **10**, Table 2), while compounds containing fluorine atom(s) at position *ortho* and *para* (**9**) or *para* (**8**) at the phenyl ring of phenylpiperazine moiety displayed higher affinity for  $\alpha_1$ -ARs ( $K_i = 42.0, 44.0$  nM, respectively) than compound **7** possessing an *o*-fluorophenylpiperazine moiety ( $K_i = 100$  nM). The molecular geometry of these compounds in the crystals is very similar (Figure 4). Our research also indicated that the substituents at position *meta*, *ortho* and *meta* or *meta* and *para* of the phenylpiperazine phenyl ring seem to be unfavorable. The obtained results are in agreement with the previously drawn conclusion that the methoxy group at *o*-position at the phenyl ring of

phenylpiperazine moiety is favorable for the affinity to  $\alpha_1$ -ARs [39,41,42,45,47,54–57]. In the case of the linker, a long carbon chain consisting of 6 carbon atoms seems to have a beneficial influence on affinity to  $\alpha_1$ -ARs of an *o*-methoxyphenylpiperazine derivative.

The intrinsic activity assay enabled the determination of agonist/antagonist profile as well as selectivity towards  $\alpha_{1A}$ - and  $\alpha_{1B}$ -ARs. All selected compounds (1–3, 5–9, 11–14) showed antagonistic activity to both tested  $\alpha_1$ -AR subtypes (Table 3). Two compounds (1 and 5), both belonging to group A and possessing methoxy group at *o*-position at the phenyl ring, displayed strong ( $IC_{50} < 100$  nM)  $\alpha_{1A}$ -AR antagonistic intrinsic activity, while representatives from group B (9, 11, 13) proved moderate one ( $100$  nM  $< IC_{50} < 200$  nM). In the case of  $\alpha_{1B}$ -AR, all *o*-methoxyphenylpiperazine derivatives from group A (1 and 5) showed  $IC_{50} < 100$  nM. Nevertheless, selectivity ratio calculation revealed that 2-methoxy (13) and 2-cyano (11) group with 2-hydroxypropyl linker at the N1-position of hydantoin could be responsible for better subtype selectivity for  $\alpha_{1A}$  (over  $\alpha_{1B}$ ), while long carbon chains, first of all hexyl (5), secondly pentyl (3), linkers seem to be beneficial for the subtype selectivity for  $\alpha_{1B}$  (over  $\alpha_{1A}$ ). Furthermore, the antagonistic intrinsic activity of 5 towards  $\alpha_{1A}$  was similar to the most potent tested reference, tamsulosin (Figure 5a) and higher than all reference compounds in the case of  $\alpha_{1B}$ -AR, including tamsulosin (Figure 5b).

In vivo assay on normotensive rats was carried out in order to assess the hypotensive activity of selected compounds (1–3, 5–9, 11–14). All tested compounds possessing *o*-methoxyphenylpiperazine fragments (1, 5, 13) proved significant reduction of systolic and diastolic blood pressure as well as one with unsubstituted phenylpiperazine (3). Furthermore, these effects were observed for compound 5 in a 16-fold lower dose than for urapidil (0.0625 vs. 1.0 mg/kg, respectively). Results obtained via in vivo study correlated with in vitro functional assays. The hypotensive activity compounds showed strong antagonistic effects at  $\alpha_{1A}$ -AR (13) and/or  $\alpha_{1B}$ -AR (1, 3, 5), but the short-term, strong hypotensive effect of compound 13 may result from a different mechanism of antihypertensive action than the  $\alpha_1$ -blocker or different pharmacokinetics, which would be worth investigating at a later stage of research. Moreover, compound 5 displayed a stronger effect at  $\alpha_1$ -ARs than classic  $\alpha_1$ -AR blockers like prazosin and terazosin, well known as antihypertensive drugs [58,59]. The presented results suggested that these compounds exhibited hypotensive activity through  $\alpha_1$ -AR blockade. Analyzing the structure of the most active compound (5), it could be stated that methoxy-substituent at the ortho position of the phenyl ring and hexyl linker at the N1-position of hydantoin are very favorable in case of hypotensive effects by blocking  $\alpha_{1B}$ -AR. The identified  $\alpha_{1A}$ -AR selective antagonists also can help the design of efficacious drugs for arrhythmias. Discovery of new  $\alpha_1$ -AR antagonist (5), moderately selective for  $\alpha_{1B}$  over  $\alpha_{1A}$  subtype (10-fold), is promising for the development of novel hypotensive drugs. Moreover, among tested phenylpiperazine derivatives, compound 11 (*o*-CN-phenylpiperazine derivative) exhibited no significant changes in the hemodynamic parameters (SBP and DBP) and demonstrated in vitro strong antagonistic activity at  $\alpha_{1A}$ -AR. Moreover, this compound showed a slight selectivity for  $\alpha_{1A}$  over  $\alpha_{1B}$  subtype. This can suggest that 2-cyano- substituent at the phenyl ring of the phenylpiperazine moiety exerts a beneficial influence on  $\alpha_{1A}$  subtype selectivity (over  $\alpha_{1B}$ ). Thus, these data can aid the development of new  $\alpha_{1A}$ -AR selective blockers used in the treatment of patients with BPH/LUTS.

## 4. Materials and Methods

### 4.1. Chemistry

Reagents were purchased from Alfa Aesar (Karlsruhe, Germany) or Sigma Aldrich (Darmstadt, Germany). Reaction progress was verified using thin layer chromatography (TLC), which was carried out on 0.2 mm Merck silica gel 60 F254 plates. Spots were visualized by UV light. Melting points (m.p.) were determined using the MEL-TEMP II apparatus (LD Inc., Long Beach, CA, USA) and were uncorrected. The  $^1H$ -NMR spectra were obtained on a Mercury-VX 300 Mz spectrometer (Varian, Palo Alto, CA, USA) in DMSO- $d_6$ . Chemical shifts in  $^1H$ -NMR spectra were reported in parts per million (ppm)

on the  $\delta$  scale using the solvent signal as an internal standard. Data are reported as follows: chemical shift, multiplicity (s, singlet; d, doublet; dd—doublet of doublets; t, triplet; m, multiplet), coupling constant  $J$  in Hertz (Hz), number of protons, proton's position (Im—imidazolone, Benz—benzyl, Ph—phenyl, Pp—piperazine). Mass spectra were recorded on a UPLC-MS/MS system consisting of a Waters ACQUITY®UPLC® (Waters Corporation, Milford, MA, USA) coupled to a Waters TQD mass spectrometer (electrospray ionization mode ESI-tandem quadrupole). Chromatographic separations were carried out using the Acquity UPLC BEH (bridged ethyl hybrid) C18 column;  $2.1 \times 100$  mm, and  $1.7 \mu\text{m}$  particle size, equipped with Acquity UPLC BEH C18 VanGuard precolumn (Waters Corporation, Milford, MA, USA);  $2.1 \times 5$  mm, and  $1.7 \mu\text{m}$  particle size. The column was maintained at  $40^\circ\text{C}$  and eluted under gradient conditions from 95% to 0% of eluent A over 10 min, at a flow rate of  $0.3 \text{ mL}\cdot\text{min}^{-1}$ . Eluent A: water/formic acid (0.1%, *v/v*); eluent B: acetonitrile/formic acid (0.1%, *v/v*). Chromatograms were made using Waters eL PDA detector. Spectra were analyzed in the 200–700 nm range with 1.2 nm resolution and a sampling rate 20 points/s. MS detection settings of Waters TQD mass spectrometer were as follows: source temperature  $150^\circ\text{C}$ , desolvation temperature  $350^\circ\text{C}$  desolvation gas flow rate  $600 \text{ L}\cdot\text{h}^{-1}$ , cone gas flow  $100 \text{ L}\cdot\text{h}^{-1}$ , capillary potential 3.00 kV, cone potential 40 V. Nitrogen was used for both nebulizing and drying gas. The data were obtained in a scan mode ranging from 50 to 1000  $m/z$  in time 0.5 s intervals. The data acquisition software was MassLynx V 4.1 (Waters Corporation, Milford, MA, USA). The UPLC/MS purity of all the final compounds was confirmed to be 95% or higher. Retention times ( $t_R$ ) are given in minutes. The UPLC/MS purity of all final compounds was determined (%). Syntheses under microwave irradiation were performed in a household microwave oven Samsung MW71B. Synthesis of compounds 7–9, 15, 16, 18–20 was described earlier [48,50], and the procedure for intermediate 17 can be found in Supplementary Materials.

#### 4.1.1. General Procedure to Obtain Final Products from Group A (1–5)

Piperazine derivatives (2–4 mmol), potassium carbonate (6.5–13.0 mmol, 0.9–1.80 g), acetone (7.5–15.0 mL), and 2,4-dichlorobenzyl-1-bromoalkyl-5,5-dimethylimidazolidine-2,4-dione derivatives (17–19) (4.0–8.0 mmol) dissolved in acetone (10.0–15.0 mL) were heated at reflux for 3.75–11 h. Then, filtration was carried out. The filtrate was evaporated. To the residue, dichloromethane was added, and it was washed 2–3 times with 1% HCl. Organic fractions were dried, then filtrated and evaporated. Solid products were obtained using method A-B. Method A—Saturation using gaseous hydrochloric acid; Method B—When method A was unsuccessful, the obtained compound was dissolved in anhydrous ethanol, and diethyl ether was added. It was mixed for 30 min and then put into the refrigerator for 2–7 days. Then, filtration was performed. Method C: If the solid product from method A or B was impure, it was heated in acetone for 5 min. The suspension was put into the fridge for 15 min and then into the refrigerator for an additional 15 min. Finally, Buchner filtration was conducted to obtain a pure product.

3-(2,4-dichlorobenzyl)-1-(3-(4-(2-methoxyphenyl)piperazin-1-yl)propyl)-5,5-dimethylimidazolidine-2,4-dione hydrochloride (1).

1-(2-methoxyphenyl)piperazine (4 mmol, 0.77 g) and the 3-bromopropyl derivative (17) (8.0 mmol, 3.2 g) were used. Product was obtained using method A. White solid. Yield 60.0%; mp  $201\text{--}203^\circ\text{C}$ .  $\text{C}_{26}\text{H}_{33}\text{Cl}_3\text{N}_4\text{O}_2$  MW 555.93. LC/MS±: purity 98.64%  $t_R = 5.60$ , (ESI)  $m/z$  [M + H] 519.12.  $^1\text{H}$  NMR (DMSO- $d_6$ , ppm):  $\delta$  10.67 (s, 1H,  $\text{NH}^+$ ), 7.66 (d,  $J = 2.1$  Hz, 1H, Benz-3-H), 7.43 (dd,  $J = 8.4, 2.2$  Hz, 1H, Benz-5-H), 7.21 (d,  $J = 8.4$  Hz, 1H, Benz-6-H), 7.07–6.86 (m, 4H, PpPh-3,4,5,6-H), 4.63 (s, 2H, N3- $\text{CH}_2$ ), 3.79 (s, 3H,  $\text{OCH}_3$ ), 3.60–3.34 (m, 6H, Pp-3,5-H, N1- $\text{CH}_2$ ), 3.25–2.97 (m, 6H, Pp-2,6-H, Pp- $\text{CH}_2$ ), 2.13–1.95 (m, 2H, Pp- $\text{CH}_2\text{-CH}_2$ ), 1.42 (s, 6H,  $2 \times \text{Im-CH}_3$ ).

3-(2,4-dichlorobenzyl)-1-(3-(4-(2,3-dichlorophenyl)piperazin-1-yl)propyl)-5,5-dimethylimidazolidine-2,4-dione hydrochloride (2).

1-(2,3-dichlorophenyl)piperazine (4 mmol, 0.92 g) and the 3-bromopropyl derivative (17) (8.0 mmol, 3.2 g) were used. The product was obtained using method B. White

solid. Yield 62.0%; mp 185–187 °C. C<sub>25</sub>H<sub>29</sub>Cl<sub>5</sub>N<sub>4</sub>O<sub>2</sub> MW 594.78. LC/MS±: purity 97.84% t<sub>R</sub> = 6.48, (ESI) *m/z* [M + H] 559.00. <sup>1</sup>H NMR (DMSO-d<sub>6</sub>, ppm): δ 10.73 (s, 1H, NH<sup>+</sup>), 7.64 (d, *J* = 2.1 Hz, 1H, Benz-3-H), 7.44–7.29 (m, 3H, Benz-5,6-H, PpPh-4-H), 7.23–7.17 (m, 2H, PpPh-5,6-H), 4.61 (s, 2H, N3-CH<sub>2</sub>), 3.56 (d, *J* = 5.9 Hz, 2H, Pp-3,5-H<sub>b</sub>), 3.47–3.31 (m, 4H, N1-CH<sub>2</sub>, Pp-3,5-H<sub>a</sub>), 3.25–3.05 (m, 6H, Pp-CH<sub>2</sub>, Pp-2,6-H), 2.12–1.92 (m, 2H, Pp-CH<sub>2</sub>-CH<sub>2</sub>), 1.38 (s, 6H, 2 × Im-CH<sub>3</sub>).

3-(2,4-dichlorobenzyl)-5,5-dimethyl-1-(5-(4-phenylpiperazin-1-yl)pentyl)imidazolidine-2,4-dione hydrochloride (3).

1-phenylpiperazine (4 mmol, 0.65 g) and the 3-bromopentyl derivative (18) (5 mmol, 2.18 g) were used. The product was obtained using method A. White solid. Yield 37.5%; mp 218–220 °C. C<sub>27</sub>H<sub>35</sub>Cl<sub>3</sub>N<sub>4</sub>O<sub>2</sub> MW 553.95. LC/MS±: purity 100.00% t<sub>R</sub> = 5.90, (ESI) *m/z* [M + H] 517.13. <sup>1</sup>H NMR (DMSO-d<sub>6</sub>, ppm): δ 10.49 (s, 1H, NH<sup>+</sup>), 7.65 (d, *J* = 2.1 Hz, 1H, Benz-3-H), 7.43 (dd, *J* = 8.4, 2.2 Hz, 1H, Benz-5-H), 7.31–7.22 (m, 2H, PpPh-3,5-H), 7.18 (d, *J* = 8.4 Hz, 1H, Benz-6-H), 7.00 (d, *J* = 7.9 Hz, 2H, PpPh-2,6-H), 6.86 (t, *J* = 7.3 Hz, 1H, PpPh-4-H), 4.62 (s, 2H, N3-CH<sub>2</sub>), 3.88–3.44 (m, 4H, Pp-3,5-H), 3.28 (t, *J* = 7.4 Hz, 2H, N1-CH<sub>2</sub>), 3.19–3.00 (m, 6H, Pp-CH<sub>2</sub>, Pp-2,6-H), 1.83–1.68 (m, 2H, N1-CH<sub>2</sub>CH<sub>2</sub>), 1.68–1.54 (m, 2H, Pp-CH<sub>2</sub>CH<sub>2</sub>), 1.38 (s, 6H, 2 × Im-CH<sub>3</sub>), 1.36–1.29 (m, 2H, PpCH<sub>2</sub>CH<sub>2</sub>CH<sub>2</sub>).

3-(2,4-dichlorobenzyl)-1-(6-(4-(3,4-dichlorophenyl)piperazin-1-yl)hexyl)-5,5-dimethylimidazolidine-2,4-dione hydrochloride (4).

1-(3,4-dichlorophenyl)piperazine (2 mmol, 0.46 g) and the 3-bromohexyl derivative (19) (4.0 mmol, 1.80 g) were used. Product was obtained using methods B and C. White solid. Yield 2.0%; mp 154–156 °C. C<sub>28</sub>H<sub>35</sub>Cl<sub>5</sub>N<sub>4</sub>O<sub>2</sub> MW 636.86. LC/MS±: purity 99.10% t<sub>R</sub> = 6.84, (ESI) *m/z* [M + H] 601.46. <sup>1</sup>H NMR (DMSO-d<sub>6</sub>, ppm): δ 11.09 (s, 1H, NH<sup>+</sup>), 7.64 (d, *J* = 2.1 Hz, 1H, Benz-3-H), 7.50–7.37 (m, 2H, Benz-5-H, Ph-5-H), 7.24 (d, *J* = 2.8 Hz, 1H, Ph-2-H), 7.17 (d, *J* = 8.4 Hz, 1H, Benz-6-H), 7.00 (dd, *J* = 9.0, 2.8 Hz, 1H, Ph-6-H), 4.61 (s, 2H, N3-CH<sub>2</sub>), 3.95–3.80 (m, 2H, Pp-3,5-H<sub>b</sub>), 3.58–3.43 (m, 2H, Pp-3,5-H<sub>a</sub>), 3.35–3.16 (m, 4H, N1-CH<sub>2</sub>, Pp-CH<sub>2</sub>), 3.14–2.97 (m, 4H, Pp-2,6-H), 1.84–1.66 (m, 2H, Pp-CH<sub>2</sub>CH<sub>2</sub>), 1.66–1.50 (m, 2H, N1-CH<sub>2</sub>CH<sub>2</sub>), 1.44–1.26 (m, 10H, N1-CH<sub>2</sub>CH<sub>2</sub>CH<sub>2</sub>, Pp-CH<sub>2</sub>CH<sub>2</sub>CH<sub>2</sub>, 2 × Im-CH<sub>3</sub>).

3-(2,4-dichlorobenzyl)-1-(6-(4-(2-methoxyphenyl)piperazin-1-yl)hexyl)-5,5-dimethylimidazolidine-2,4-dione hydrochloride (5).

1-(2-methoxyphenyl)piperazine (2 mmol, 0.38 g) and the 3-bromohexyl derivative (19) (4.0 mmol, 1.80 g) were used. Product was obtained using methods A and C. White solid. Yield 45.0%; mp 205–207 °C. C<sub>29</sub>H<sub>39</sub>Cl<sub>3</sub>N<sub>4</sub>O<sub>3</sub> MW 598.01. LC/MS±: purity 95.67% t<sub>R</sub> = 6.19, (ESI) *m/z* [M + H] 562.26. <sup>1</sup>H NMR (DMSO-d<sub>6</sub>, ppm): δ 11.02 (s, 1H, NH<sup>+</sup>), 7.65 (d, *J* = 2.1 Hz, 1H, Benz-3-H), 7.43 (dd, *J* = 8.3, 2.2 Hz, 1H, Benz-5-H), 7.17 (d, *J* = 8.4 Hz, 1H, Benz-6-H), 7.06–6.87 (m, 4H, PpPh-3,4,5,6-H), 4.62 (s, 2H, N3-CH<sub>2</sub>), 3.80 (s, 3H, OCH<sub>3</sub>), 3.58–3.39 (m, 4H, Pp-3,5-H), 3.31–3.20 (m, 2H, N1-CH<sub>2</sub>), 3.20–3.00 (m, 6H, Pp-CH<sub>2</sub>, Pp-2,6-H), 1.82–1.66 (m, 2H, Pp-CH<sub>2</sub>CH<sub>2</sub>), 1.66–1.50 (m, 2H, N1-CH<sub>2</sub>CH<sub>2</sub>), 1.45–1.26 (m, 10H, N1-CH<sub>2</sub>CH<sub>2</sub>CH<sub>2</sub>, Pp-CH<sub>2</sub>CH<sub>2</sub>CH<sub>2</sub>, 2 × Im-CH<sub>3</sub>).

#### 4.1.2. General Procedure to Obtain Final Products from Group B (6, 10–14)

Piperazine derivatives (3 mmol) and the 3-(2,4-dichlorobenzyl)-5,5-dimethyl-1-(oxiran-2-ylmethyl)imidazolidine-2,4-dione (20) (3 mmol) were dissolved in acetone (15–20 mL). The mixture was evaporated and irradiated in a household microwave (300–450 W) for 3–7 min. Crystallization using ethanol anhydrous was conducted. Method A: Solid products were obtained through saturation using gaseous hydrochloric acid. Method B: When method A was unsuccessful, the obtained compound was dissolved in anhydrous ethanol, and diethyl ether was added. It was stirred for 30 min and then put into the refrigerator for 2–7 days. Then, filtration was carried out. In order to obtain pure product, crystallization from acetone was carried out.

3-(2,4-dichlorobenzyl)-1-(2-hydroxy-3-(4-phenylpiperazin-1-yl)propyl)-5,5-dimethylimidazolidine-2,4-dione hydrochloride (6).

1-phenylpiperazine (3 mmol, 0.49 g) and 3-(2,4-dichlorobenzyl)-5,5-dimethyl-1-(oxiran-2-ylmethyl)imidazolidine-2,4-dione (**20**) (3.0 mmol, 1.03 g) were used. The product was obtained using method B. White solid. Yield 89.0%; mp 196–198 °C. C<sub>25</sub>H<sub>31</sub>Cl<sub>3</sub>N<sub>4</sub>O<sub>3</sub> MW 541.90. LC/MS±: purity 99.45% t<sub>R</sub> = 6.60, (ESI) *m/z* [M + H] 506.44. <sup>1</sup>H NMR (DMSO-d<sub>6</sub>, ppm): δ 10.74 (s, 1H, NH<sup>+</sup>), 7.64 (d, *J* = 2.1 Hz, 1H, Benz-3-H), 7.42 (dd, *J* = 8.4, 2.2 Hz, 1H, Benz-5-H), 7.31–7.21 (m, 3H, Benz-6-H, Ph-3,5-H), 7.00 (d, *J* = 7.9 Hz, 2H, Ph-2,6-H), 6.86 (t, *J* = 7.3 Hz, 1H, Ph-4-H), 4.63 (s, 2H, N3-CH<sub>2</sub>), 4.45–4.33 (m, *J* = 7.3 Hz, 1H, CH-OH), 3.93–3.01 (m, 12H, Pp-2,3,5,6-H, Pp-CH<sub>2</sub>, N1-CH<sub>2</sub>), 1.44 (s, 3H, 2 × Im-CH<sub>3b</sub>), 1.41 (s, 3H, 2 × Im-CH<sub>3a</sub>).

3-(2,4-dichlorobenzyl)-1-(3-(4-(3,4-dichlorophenyl)piperazin-1-yl)-2-hydroxypropyl)-5,5-dimethylimidazolidine-2,4-dione hydrochloride (**10**).

1-(3,4-dichlorophenyl)piperazine (3 mmol, 0.69 g) and 3-(2,4-dichlorobenzyl)-5,5-dimethyl-1-(oxiran-2-ylmethyl)imidazolidine-2,4-dione (**20**) (3.0 mmol, 1.03 g) were used. The product was obtained using method A. White solid. Yield 4.0%; mp 223–225 °C. C<sub>25</sub>H<sub>29</sub>Cl<sub>5</sub>N<sub>4</sub>O<sub>3</sub> MW 610.78. LC/MS±: purity 97.61% t<sub>R</sub> = 6.29, (ESI) *m/z* [M + H] 575.33. <sup>1</sup>H NMR (DMSO-d<sub>6</sub>, ppm): δ 10.56 (s, 1H, NH<sup>+</sup>), 7.65 (d, *J* = 2.0 Hz, 1H, Benz-3-H), 7.50–7.38 (m, 2H, Benz-5-H, PpPh-5-H), 7.31–7.21 (m, 2H, Benz-6-H, PpPh-2-H), 7.00 (dd, *J* = 9.0, 2.5 Hz, 1H, PpPh-6-H), 5.94 (s, 1H, OH), 4.63 (s, 2H, N3-CH<sub>2</sub>), 4.48–4.24 (m, 1H, CH-OH), 4.04–3.77 (m, 2H, N1-CH<sub>2</sub>), 3.75–3.35 (m, 4H, Pp-3,5-H), 3.30–2.97 (m, 6H, Pp-2,6-H, Pp-CH<sub>2</sub>), 1.43 (s, 3H, Im-CH<sub>3b</sub>), 1.41 (s, 3H, Im-CH<sub>3a</sub>).

3-(2,4-dichlorobenzyl)-1-(3-(4-(2-cyanophenyl)piperazin-1-yl)-2-hydroxypropyl)-5,5-dimethylimidazolidine-2,4-dione hydrochloride (**11**).

1-(2-cyanophenyl)piperazine (3 mmol, 0.56 g) and 3-(2,4-dichlorobenzyl)-5,5-dimethyl-1-(oxiran-2-ylmethyl)imidazolidine-2,4-dione (**20**) (3.0 mmol, 1.03 g) were used. The product was obtained using method A. Cream solid. Yield 25.0%; mp 147–149 °C. C<sub>26</sub>H<sub>30</sub>Cl<sub>3</sub>N<sub>5</sub>O<sub>3</sub> MW 566.91. LC/MS±: purity 100.00% t<sub>R</sub> = 5.46, (ESI) *m/z* [M + H] 531.45.

<sup>1</sup>H NMR (DMSO-d<sub>6</sub>, ppm): δ 10.66 (s, 1H, NH<sup>+</sup>), 7.76 (dd, *J* = 7.7, 1.5 Hz, 1H, PpPh-3-H), 7.69–7.60 (m, 2H, PpPh-5-H, Benz-3-H), 7.43 (dd, *J* = 8.4, 2.2 Hz, 1H, Benz-5-H), 7.26 (m, 2H, Benz-6-H, PpPh-6-H), 7.18 (t, *J* = 7.6 Hz, 1H, PpPh-4-H), 5.94 (s, 1H, OH), 4.64 (s, 2H, N3-CH<sub>2</sub>), 4.38 (s, 1H, CH-OH), 3.81–3.50 (m, 4H, N1-CH<sub>2</sub>, Pp-3,5-H<sub>a</sub>), 3.46–3.04 (m, 8H, Pp-3,5-H<sub>b</sub>, Pp-2,6-H, Pp-CH<sub>2</sub>), 1.44 (s, 3H, Im-CH<sub>3b</sub>), 1.42 (s, 3H, Im-CH<sub>3a</sub>).

3-(2,4-dichlorobenzyl)-1-(3-(4-(3,4-dimethylphenyl)piperazin-1-yl)-2-hydroxypropyl)-5,5-dimethylimidazolidine-2,4-dione hydrochloride (**12**).

1-(3,4-dimethylphenyl)piperazine (3 mmol; 0.57 g) and 3-(2,4-dichlorobenzyl)-5,5-dimethyl-1-(oxiran-2-ylmethyl)imidazolidine-2,4-dione (**20**) (3.0 mmol; 1.03 g) were used. The product was obtained using method A. White solid. Yield 89.0%; mp 217–219 °C. C<sub>27</sub>H<sub>35</sub>Cl<sub>3</sub>N<sub>4</sub>O<sub>3</sub> MW 569.95. LC/MS±: purity 97.44% t<sub>R</sub> = 5.92; (ESI) *m/z* [M + H] 534.49. <sup>1</sup>H NMR (DMSO-d<sub>6</sub>; ppm): δ 10.56 (s; 1H; NH<sup>+</sup>), 7.64 (d; *J* = 2.1 Hz; 1H; Benz-3-H); 7.42 (dd; *J* = 8.4; 2.2 Hz; 1H; Benz-5-H); 7.25 (d; *J* = 8.4 Hz; 1H; Benz-6-H); 7.00 (d; *J* = 8.3 Hz; 1H; PpPh-5-H); 6.80 (d; *J* = 2.3 Hz; 1H; PpPh-2-H); 6.70 (dd; *J* = 8.2; 2.5 Hz; 1H; PpPh-6-H); 6.07–5.85 (m; 1H; OH); 4.63 (s; 2H; N3-CH<sub>2</sub>); 4.45–4.31 (m; 1H; CH-OH); 3.85–2.99 (m; 12H; N1-CH<sub>2</sub>, Pp-2,3,5,6-H; Pp-CH<sub>2</sub>); 2.19 (s; 3H; PpPh-3-CH<sub>3</sub>); 2.11 (s; 3H; PpPh-4-CH<sub>3</sub>); 1.44 (s; 3H; Im-CH<sub>3b</sub>); 1.42 (s; 3H; Im-CH<sub>3a</sub>).

3-(2,4-dichlorobenzyl)-1-(2-hydroxy-3-(4-(2-methoxyphenyl)piperazin-1-yl)propyl)-5,5-dimethylimidazolidine-2,4-dione hydrochloride (**13**).

1-(2-methoxyphenyl)piperazine (3 mmol, 0.58 g) and 3-(2,4-dichlorobenzyl)-5,5-dimethyl-1-(oxiran-2-ylmethyl)imidazolidine-2,4-dione (**20**) (3.0 mmol, 1.03 g) were used. Product was obtained using method A. White solid. Yield 36.0%; mp 144–146 °C. C<sub>26</sub>H<sub>33</sub>Cl<sub>3</sub>N<sub>4</sub>O<sub>4</sub> MW 571.92. LC/MS±: purity 97.54% t<sub>R</sub> = 5.48, (ESI) *m/z* [M + H] 536.46. <sup>1</sup>H NMR (DMSO-d<sub>6</sub>, ppm): δ 10.62 (s, 1H, NH<sup>+</sup>), 7.65 (d, *J* = 2.1 Hz, 1H, Benz-3-H), 7.42 (dd, *J* = 8.4, 2.1 Hz, 1H, Benz-5-H), 7.26 (d, *J* = 8.4 Hz, 1H, Benz-6-H), 7.07–6.86 (m, 4H, PpPh-3,4,5,6-H), 5.86 (s, 1H, OH), 4.63 (s, 2H, N3-CH<sub>2</sub>), 4.46–4.30 (m, 1H, CH-OH), 3.79 (s, 3H, OCH<sub>3</sub>), 3.73–3.01 (m, 12H, N1-CH<sub>2</sub>, Pp-2,3,5,6-H, Pp-CH<sub>2</sub>), 1.45 (s, 3H, Im-CH<sub>3b</sub>), 1.42 (s, 3H, Im-CH<sub>3a</sub>).

3-(2,4-dichlorobenzyl)-1-(2-hydroxy-3-(4-(3-methoxyphenyl)piperazin-1-yl)propyl)-5,5-dimethylimidazolidine-2,4-dione hydrochloride (**14**).

1-(3-methoxyphenyl)piperazine (3 mmol, 0.58 g) and 3-(2,4-dichlorobenzyl)-5,5-dimethyl-1-(oxiran-2-ylmethyl)imidazolidine-2,4-dione (**20**) (3.0 mmol, 1.03 g) were used. The product was obtained using method A. White solid. Yield 38.0%; mp 177–179 °C.  $C_{26}H_{33}Cl_3N_4O_4$  MW 571.92. LC/MS±: purity 100.00%  $t_R = 5.45$ , (ESI)  $m/z$  [M + H] 536.46.  $^1H$  NMR (DMSO- $d_6$ , ppm):  $\delta$  10.59 (s, 1H,  $NH^+$ ), 7.65 (d,  $J = 2.1$  Hz, 1H, Benz-3-H), 7.42 (dd,  $J = 8.4, 2.2$  Hz, 1H, Benz-5-H), 7.25 (d,  $J = 8.4$  Hz, 1H, Benz-6-H), 7.15 (t,  $J = 8.2$  Hz, 1H, PpPh-5-H), 6.57 (dd,  $J = 8.2, 2.0$  Hz, 1H, PpPh-6-H), 6.52 (t,  $J = 2.2$  Hz, 1H, PpPh-2-H), 6.44 (dd,  $J = 8.1, 2.0$  Hz, 1H, PpPh-4-H), 6.02–5.89 (m, 1H, OH), 4.63 (s, 2H,  $N3-CH_2$ ), 4.45–4.31 (m, 1H, CH-OH), 3.91–3.00 (m, 15H,  $OCH_3$ ,  $N1-CH_2$ , Pp-2,3,5,6-H, Pp- $CH_2$ ), 1.44 (s, 3H, Im- $CH_{3b}$ ), 1.42 (s, 3H, Im- $CH_{3a}$ ).

#### 4.2. Crystallography

Crystals suitable for an X-ray structure analysis were grown from n-butyl acetate for **7**, while for **8** and **9** from n-propyl acetate, by slow evaporation of the solvent at room temperature.

Data for single crystals of **7** and **9** were collected at 130K using the Oxford Diffraction SuperNova four-circle diffractometer equipped with the Mo (0.71073 Å)  $K\alpha$  radiation source, graphite monochromator, while for **8** were collected using the XtaLAB Synergy-S diffractometer, equipped with the Cu (1.54184 Å)  $K\alpha$  radiation source and graphite monochromator. Positions of all non-hydrogen atoms were determined by direct methods using the SIR-2014 [60] program. Refinement and further calculations were carried out using the SHELXL-2018 program [61]. All non-hydrogen atoms were refined anisotropically using weighted full-matrix least-squares on  $F^2$ . The hydrogen atoms attached to oxygen atoms were identified on different Fourier maps, whereas all hydrogen atoms bonded to carbon atoms were included in the structure at idealized positions and were refined using a riding model with  $U_{iso}$  (H) fixed at 1.2  $U_{eq}$  of C and 1.5  $U_{eq}$  for methyl groups. In the crystal structures of **7** and **9**, a water molecule is present in the crystal lattice, wherein for **9** the occupancy factor of 0.3 of water molecule was used for refinement, and for molecular graphics, the MERCURY [62] program was used.

**7**:  $C_{25}H_{30}Cl_2FO_3N_4^+Cl^- \cdot H_2O$ , Mr = 577.89, crystal size =  $0.12 \times 0.21 \times 0.49$  mm<sup>3</sup>, triclinic, space group  $P\bar{1}$ , a = 7.9131(3) Å, b = 13.0967(5) Å, c = 14.1077(5) Å,  $\alpha = 68.230(3)^\circ$ ,  $\beta = 82.945(3)^\circ$ ,  $\gamma = 86.697(3)^\circ$ , V = 1347.4(1) Å<sup>3</sup>, Z = 2, T = 130(2) K, 18,567 reflections collected, 6279 unique reflections (Rint = 0.0260), R1 = 0.0532, wR2 = 0.1416 [ $I > 2\sigma(I)$ ] and R1 = 0.0683, wR2 = 0.1551 [all data].

**8**:  $C_{25}H_{30}Cl_2FO_3N_4^+Cl^-$ , Mr = 559.88, crystal size =  $0.07 \times 0.17 \times 0.30$  mm<sup>3</sup>, triclinic, space group  $P\bar{1}$ , a = 7.8606(1) Å, b = 13.0752(2) Å, c = 14.4597(2) Å,  $\alpha = 64.936(2)^\circ$ ,  $\beta = 81.780(1)^\circ$ ,  $\gamma = 88.492(1)^\circ$ , V = 1331.4(4) Å<sup>3</sup>, Z = 2, T = 100(2) K, 36,993 reflections collected, 5449 unique reflections (Rint = 0.0439), R1 = 0.0401, wR2 = 0.1036 [ $I > 2\sigma(I)$ ] and R1 = 0.0421, wR2 = 0.1052 [all data].

**9**:  $C_{25}H_{30}Cl_2F_2O_3N_4^+Cl^- \cdot 0.3H_2O$ , Mr = 583.28, crystal size =  $0.26 \times 0.45 \times 0.85$  mm<sup>3</sup>, triclinic, space group  $P\bar{1}$ , a = 7.9118(3) Å, b = 13.0975(4) Å, c = 14.4313(5) Å,  $\alpha = 65.905(2)^\circ$ ,  $\beta = 81.045(3)^\circ$ ,  $\gamma = 88.293(3)^\circ$ , V = 1347.56(9) Å<sup>3</sup>, Z = 2, T = 130(2) K, 18,752 reflections collected, 6313 unique reflections (Rint = 0.0228), R1 = 0.0503, wR2 = 0.1250 [ $I > 2\sigma(I)$ ] and R1 = 0.0630, wR2 = 0.1348 [all data].

CCDC 2248728–2248730 contains the supplementary crystallographic data. These data can be obtained free of charge from The Cambridge Crystallographic Data Centre via [www.ccdc.cam.ac.uk/data\\_request/cif](http://www.ccdc.cam.ac.uk/data_request/cif) (accessed on 14 March 2023).

#### 4.3. Pharmacology

##### 4.3.1. Chemicals

The following drugs and chemicals were used: thiopental (Rotexmedica, Trittau, Germany), heparin 5000 IU/mL (WZF Polfa S.A., Warsaw, Poland), ethyl alcohol 99.9%

(Chempur, Piekary Śląskie, Poland), kolliphor (Sigma-Aldrich, Taufkirchen, Germany), sodium chloride (POCH, Gliwice, Poland), urapidil hydrochloride (Sigma-Aldrich, Germany), prazosin hydrochloride (Sigma-Aldrich, Germany), terazosin hydrochloride (Sigma-Aldrich, Germany), tamsulosin hydrochloride (Sigma-Aldrich, Germany), and phenylephrine (Sigma-Aldrich, Germany).

#### 4.3.2. Animals

The experiments were carried out on male normotensive Wistar rats (outbred stock, name: KRF:WI(WU)) weighing 250 to 300 g. The animals were purchased from a licensed breeder (Animal House, Faculty of Pharmacy, Jagiellonian University Medical College, Krakow, Poland). The rats were housed in pairs in standard plastic cages at a constant room temperature of 22–24 °C, relative humidity of 55 ± 10%, with a 12:12 h light/dark cycle (light on from 7 a.m. to 7 p.m.). The animals had free access to food pellets (Agropol S.J., Motycz, Poland) and filtered tap water. The experimental groups consisted of six animals each. The rats were adopted for 5 days to the laboratory conditions before being used in experiments. The animals were killed by cervical dislocation immediately after the experiments. All experimental procedures were performed according to the European Union Directive of 22 September 2010 (2010/63/EU) and Polish legislation concerning animal care and use and approved by the 2nd Local Ethics Committee for Experiments on Animals in Krakow, Poland (Resolution No. 127/2017).

#### 4.3.3. In Vitro Binding Assay—Determination of Affinity for $\alpha_1$ -ARs

The affinity for  $\alpha_1$ -ARs was determined by radioligand binding assay on rat cerebral cortex using [3H]-prazosin as a specific radioligand. The brains were homogenized in 20 volumes of an ice-cold 50 mM Tris-HCl buffer (pH 7.6) and were centrifuged (MPW Med. Instruments, Warsaw, Poland) at 20,000 × *g* for 20 min (0–4 °C). The cell pellet was resuspended in the Tris-HCl buffer and centrifuged again. Radioligand-binding assay was performed in plates (MultiScreen/Millipore, Burlington, MA, USA). The final incubation mixture (final volume 300 µL) consisted of 240 µL of the membrane suspension, 30 µL of [3H]-Prazosin (0.2 nM) solution, and 30 µL of the buffer containing seven to eight concentrations ( $10^{-11}$  to  $10^{-4}$  M) of the tested compounds. For measuring the unspecific binding, phentolamine, 10 µM (in the case of [3H]-Prazosin) was applied. The incubation was terminated by rapid filtration over glass fiber filters (Whatman GF/C, Sigma-Aldrich) using a vacuum manifold (Millipore). The filters were then washed twice with the assay buffer and placed in scintillation vials with a liquid-scintillation cocktail. Radioactivity was measured in a WALLAC 1409 DSA liquid-scintillation counter (BioSurplus, San Diego, CA, USA).

#### 4.3.4. In Vitro Functional Assays—Determination of Intrinsic Activity at the $\alpha_{1A}$ -ARs and the $\alpha_{1B}$ -ARs

Intrinsic activity at the  $\alpha_1$ -AR subtypes studies were performed using the cells expressing mitochondrially-targeted aequorin and one of the human adrenergic receptor  $\alpha_{1A}$  or  $\alpha_{1B}$  (PerkinElmer, Boston, MA, USA), according to the manufacturer's instructions. For measurement, frozen cells were thawed and re-suspended in 10 mL of assay buffer containing 5 µM "Coelenterazine h". This cell suspension was put in a 10 mL Falcon tube, fixed onto a rotating heel, and incubated overnight at rt in the dark (8 rpm; 45° angle). Cells were diluted with Assay Buffer to 5000 cells/20 µL. Agonistic ligands 2 × (50 µL/well), diluted in Assay Buffer, were prepared in  $\frac{1}{2}$  white polystyrene area plates, and the cell suspension was dispensed in 50 µL volume on the ligands using the injector. The light emitted was recorded for 20 s. Cells with antagonists were incubated for 15 min at room temperature. Thereafter, 50 µL of the reference agonist phenylephrine (3 × EC<sub>80</sub> final concentration) was injected into the mix of cells and antagonist, and the light emitted was recorded for 20 s. Luminescence was measured using the multidetection microplate reader (POLARstar Omega, BMG LABTECH, Ortenberg, Germany).

#### 4.3.5. Influence on Blood Pressure in Normotensive Rats

The normotensive rats were anesthetized with thiopental (75 mg/kg) by intraperitoneal injection (i.p.). The left carotid artery was cannulated with a polyethylene tub filled with heparin in saline to facilitate pressure measurements using a PowerLab Apparatus (ADInstruments, Sydney, Australia). Blood pressure was measured immediately before administration of the tested compounds or vehicle—time 0 min (initial blood pressure) and 60 min thereafter. Initial blood pressure before administration of the tested chemicals in all experimental groups was similar. The tested compounds were dissolved in a specific vehicle: ethyl alcohol 5% – kolliphor 5% – water 90%. All tested chemicals were administered intravenously (i.v.) at a constant volume of 1 mL/kg after 20 min of stabilization period. The compounds were tested at a starting dose of 2 mg/kg. If the hypotensive activity was found, the dose was reduced by half. The dosing was continued until the hypotensive effects disappeared. Urapidil was used as a reference compound.

#### 4.3.6. Statistical Analysis

All statistics were performed using GraphPad Prism, Version 6.0 (GraphPad Software, San Diego, CA, USA). In the radioligand binding study, data were analyzed by a one-site curve-fitting equation, and inhibition constants ( $K_i$ ) values were calculated via the Cheng-Prusoff equation [63]. In functional studies, data were analyzed using a sigmoidal dose-response (variable slope) equation. Arterial blood pressure data were analyzed using a two-way ANOVA with Sidak's post-hoc test for multiple comparisons. A  $p < 0.05$  was considered statistically significant.

#### 4.4. Molecular Modelling

All the compounds were prepared for docking using LigPrep [64] from the Schrödinger Suite using default settings. Docking was carried out in Glide [65], using extra precision mode. The compounds were docked to the homology models of  $\alpha_{1A}$  and  $\alpha_{1B}$ , constructed on the basis of the GPCRdb data [66]. Homology modeling was carried out using the Modeller software version 9.13 [67] using a multi-template approach and available crystal structures of receptors from the aminergic family of GPCRs. The constructed models were evaluated by docking of known ligands and sets of inactive compounds towards  $\alpha_{1A}$  and  $\alpha_{1B}$ . For each receptor subtype, one model providing the best discrimination between active and inactive compounds (in terms of the Area Under Receiver Operating Characteristic—AUROC) was selected. Visualizations of docking poses were prepared in Pymol [68].

### 5. Conclusions

This study reported the design, synthesis and pharmacological evaluation of a series of novel phenylpiperazine derivatives of 5,5-dimethylhydantoin as  $\alpha_1$ -AR antagonists. The newly synthesized compounds showed high-to-moderate affinity for  $\alpha_1$ -ARs. Compounds containing the methoxy group at position *ortho* of the phenylpiperazine phenyl ring revealed in vitro strong antagonistic activity at  $\alpha_{1A}$ - and/or  $\alpha_{1B}$ -AR and in vivo hypotensive effects. The most promising compound (**5**) exhibited a stronger antagonistic effect at  $\alpha_{1B}$ -ARs ( $IC_{50} = 0.002$  nM) than classic  $\alpha_1$ -AR blockers such as prazosin, terazosin, tamsulosin and significantly decreased systolic and diastolic blood pressure after i.v. administration at a dose 0.0625 mg/kg. The hypotensive dose was lower than the effective dose obtained for the reference drug urapidil. Compound (**11**) possessing a 2-cyano- substituent at the phenyl ring of phenylpiperazine moiety demonstrated in vitro strong antagonistic activity at  $\alpha_{1A}$ -AR without significant changes in the hemodynamic parameters (SBP and DBP). Both compounds (**5** and **11**) are good candidates for further pharmacomodulation and biological screening development in search of innovative pharmacotherapy against circulation and urinary diseases.

**Supplementary Materials:** The following supporting information can be downloaded at: <https://www.mdpi.com/article/10.3390/ijms242316609/s1>.

**Author Contributions:** Conceptualization, J.H., M.Z., S.P., A.K. and K.K.-B.; methodology, J.H., E.Ž., M.Z., M.B., A.S., M.J.-W., W.N. and J.S.; software, S.P.; validation, S.P., A.K., J.H., K.K.-B. and M.Z.; formal analysis, S.P., K.K.-B., M.Z., J.S. and J.H.; investigation, J.K., S.P., E.Ž., M.B., A.S., M.J.-W. and W.N.; data curation, A.K. and M.Z.; writing—original draft preparation, A.K., J.K. and E.Ž.; writing—review and editing, J.H., M.Z., K.K.-B., M.B. and E.Ž.; visualization, A.K., S.P., M.Z. and E.Ž.; supervision, J.H., M.Z. and J.S.; project administration, J.H., E.Ž. and M.Z.; funding acquisition, J.H., E.Ž. and M.Z. All authors have read and agreed to the published version of the manuscript.

**Funding:** This research (crystallographic studies) was funded by the Pedagogical University of Krakow, projects number BN.711-56/PBU/2021. Chemical synthesis and pharmacological studies were supported by Jagiellonian University projects number N42/DBS/000331 and N42/DBS/000330, respectively.

**Institutional Review Board Statement:** The animal study protocols were approved by the I Local Ethics Commission in Cracow (no 127/2017, 11.04.2017) and complied with the European Communities Council Directive of 24 November 1986 (86/609/EEC) and were under the 1996 NIH Guide for the Care and Use of Laboratory Animals.

**Informed Consent Statement:** Not applicable.

**Data Availability Statement:** Data supporting reported results can be found in the Supplementary file provided during submission online.

**Acknowledgments:** Authors thank students Aleksandra Janik, Małgorzata Pycińska and Maria Glomb, who participated in the synthesis work within the Student Medicinal Chemistry Group at Jagiellonian University Medical College (SKN Chemii Medycznej UJ CM w Krakowie).

**Conflicts of Interest:** The authors declare no conflict of interest.

## References

1. Docherty, J.R. Subtypes of functional alpha1-adrenoceptor. *Cell. Mol. Life Sci.* **2010**, *67*, 405–417. [[CrossRef](#)]
2. Civantos Calzada, B.; Aleixandre de Artiñano, A. Alpha-adrenoceptor subtypes. *Pharmacol. Res.* **2001**, *44*, 195–208. [[CrossRef](#)]
3. Sriram, K.; Insel, P.A. G Protein-Coupled Receptors as Targets for Approved Drugs: How Many Targets and How Many Drugs? *Mol. Pharmacol.* **2018**, *93*, 251–258. [[CrossRef](#)]
4. Sica, D.A. Alpha1-adrenergic blockers: Current usage considerations. *J. Clin. Hypertens.* **2005**, *7*, 757–762. [[CrossRef](#)]
5. Jain, K.S.; Bariwal, J.B.; Kathiravan, M.K.; Phoujdar, M.S.; Sahne, R.S.; Chauhan, B.S.; Shah, A.K.; Yadav, M.R. Recent advances in selective alpha1-adrenoreceptor antagonists as antihypertensive agents. *Bioorganic Med. Chem.* **2008**, *16*, 4759–4800. [[CrossRef](#)]
6. Chapman, N.; Chen, C.Y.; Fujita, T.; Hobbs, F.D.; Kim, S.J.; Staessen, J.A.; Tanomsup, S.; Wang, J.G.; Williams, B. Time to re-appraise the role of alpha-1 adrenoceptor antagonists in the management of hypertension? *J. Hypertens.* **2010**, *28*, 1796–1803. [[CrossRef](#)]
7. Lepor, H.; Kazzazi, A.; Djavan, B.  $\alpha$ -Blockers for benign prostatic hyperplasia: The new era. *Curr. Opin. Urol.* **2012**, *22*, 7–15. [[CrossRef](#)]
8. Kadekawa, K.; Sugaya, K.; Ashitomi, K.; Nishijima, S. Clinical Efficacy of  $\alpha$ 1-Adrenergic Receptor Antagonist Naftopidil 75 mg/day in Patients with Benign Prostatic Hyperplasia. *Low. Urin. Tract Symptoms* **2010**, *2*, 106–112. [[CrossRef](#)]
9. Manohar, C.M.S.; Nagabhushana, M.; Karthikeyan, V.S.; Sanjay, R.P.; Kamath, A.J.; Keshavamurthy, R. Safety and efficacy of tamsulosin, alfuzosin or silodosin as monotherapy for LUTS in BPH—a double-blind randomized trial. *Cent. Eur. J. Urol.* **2017**, *70*, 148–153. [[CrossRef](#)]
10. Rudner, X.L.; Berkowitz, D.E.; Booth, J.V.; Funk, B.L.; Cozart, K.L.; D’Amico, E.B.; El-Moalem, H.; Page, S.O.; Richardson, C.D.; Winters, B.; et al. Subtype specific regulation of human vascular alpha(1)-adrenergic receptors by vessel bed and age. *Circulation* **1999**, *100*, 2336–2343. [[CrossRef](#)]
11. Adefurin, A.; Ghimire, L.V.; Kohli, U.; Muszkat, M.; Sofowora, G.G.; Li, C.; Levinson, R.T.; Paranjape, S.Y.; Stein, C.M.; Kurnik, D. Genetic variation in the alpha1B-adrenergic receptor and vascular response. *Pharm. J.* **2017**, *17*, 366–371. [[CrossRef](#)]
12. Hatano, A.; Takahashi, H.; Tamaki, M.; Komeyama, T.; Koizumi, T.; Takeda, M. Pharmacological evidence of distinct alpha 1-adrenoceptor subtypes mediating the contraction of human prostatic urethra and peripheral artery. *Br. J. Pharmacol.* **1994**, *113*, 723–728. [[CrossRef](#)]
13. Harada, K.; Ohmori, M.; Kitoh, Y.; Sugimoto, K.; Fujimura, A. A comparison of the antagonistic activities of tamsulosin and terazosin against human vascular alpha1-adrenoceptors. *Jpn. J. Pharmacol.* **1999**, *80*, 209–215. [[CrossRef](#)]
14. Jensen, B.C.; Swigart, P.M.; Montgomery, M.D.; Simpson, P.C. Functional alpha-1B adrenergic receptors on human epicardial coronary artery endothelial cells. *Naunyn Schmiedebergs Arch. Pharmacol.* **2010**, *382*, 475–482. [[CrossRef](#)]

15. Oliver, E.; Montó, F.; Rovira, E.; Valldecabres, C.; Muedra, V.; D'Ocon, P. Changes in the expression of  $\alpha$ 1B-adrenoceptor in peripheral mononuclear cells correlates with blood pressure and plasmatic homocysteine. *Biomed. Pharmacother.* **2017**, *88*, 721–727. [[CrossRef](#)]
16. Grimm, R.H., Jr.; Flack, J.M. Alpha 1 adrenoceptor antagonists. *J. Clin. Hypertens.* **2011**, *13*, 654–657. [[CrossRef](#)]
17. Black, H.R. Doxazosin as combination therapy for patients with stage 1 and stage 2 hypertension. *J. Cardiovasc. Pharmacol.* **2003**, *41*, 866–869. [[CrossRef](#)]
18. Buch, J. Urapidil, a dual-acting antihypertensive agent: Current usage considerations. *Adv. Ther.* **2010**, *27*, 426–443. [[CrossRef](#)]
19. Itskovitz, H.D. Alpha 1-blockade for the treatment of hypertension: A megastudy of terazosin in 2214 clinical practice settings. *Clin. Ther.* **1994**, *16*, 490–504.
20. Levy, D.; Walmsley, P.; Levenstein, M. Principal results of the Hypertension and Lipid Trial (HALT): A multicenter study of doxazosin in patients with hypertension. *Am. Heart J.* **1996**, *131*, 966–973. [[CrossRef](#)]
21. Dell'Omo, G.; Penno, G.; Del Prato, S.; Pedrinelli, R. Doxazosin in metabolically complicated hypertension. *Expert Rev. Cardiovasc. Ther.* **2007**, *5*, 1027–1035. [[CrossRef](#)]
22. Lehtonen, A. Doxazosin effects on insulin and glucose in hypertensive patients. The Finnish Multicenter Study Group. *Am. Heart J.* **1991**, *121 Pt 2*, 1307–1311. [[CrossRef](#)]
23. Maheux, P.; Facchini, F.; Jeppesen, J.; Greenfield, M.S.; Clinkingbeard, C.; Chen, Y.D.; Reaven, G.M. Changes in glucose, insulin, lipid, lipoprotein, and apoprotein concentrations and insulin action in doxazosin-treated patients with hypertension. Comparison between nondiabetic individuals and patients with non-insulin-dependent diabetes mellitus. *Am. J. Hypertens.* **1994**, *7*, 416–424. [[CrossRef](#)]
24. Grimm, R.H., Jr.; Flack, J.M.; Grandits, G.A.; Elmer, P.J.; Neaton, J.D.; Cutler, J.A.; Lewis, C.; McDonald, R.; Schoenberger, J.; Stamler, J. Long-term effects on plasma lipids of diet and drugs to treat hypertension. Treatment of Mild Hypertension Study (TOMHS) Research Group. *JAMA* **1996**, *275*, 1549–1556. [[CrossRef](#)]
25. Hirano, T.; Yoshino, G.; Kashiwazaki, K.; Adachi, M. Doxazosin reduces prevalence of small dense low density lipoprotein and remnant-like particle cholesterol levels in nondiabetic and diabetic hypertensive patients. *Am. J. Hypertens.* **2001**, *14 Pt 1*, 908–913. [[CrossRef](#)]
26. Kinoshita, M.; Shimazu, N.; Fujita, M.; Fujimaki, Y.; Kojima, K.; Mikuni, Y.; Horie, E.; Teramoto, T. Doxazosin, an alpha1-adrenergic antihypertensive agent, decreases serum oxidized LDL. *Am. J. Hypertens.* **2001**, *14*, 267–270. [[CrossRef](#)]
27. Derosa, G.; Cicero, A.F.; D'Angelo, A.; Ragonesi, P.D.; Ciccarelli, L.; Fogari, E.; Salvadeo, S.A.; Ferrari, I.; Gravina, A.; Fassi, R.; et al. Synergistic effect of doxazosin and acarbose in improving metabolic control in patients with impaired glucose tolerance. *Clin. Drug Investig.* **2006**, *26*, 529–539. [[CrossRef](#)]
28. Jackevicius, C.A.; Ghaznavi, Z.; Lu, L.; Warner, A.L. Safety of Alpha-Adrenergic Receptor Antagonists in Heart Failure. *JACC Heart Fail.* **2018**, *6*, 917–925. [[CrossRef](#)]
29. Perez, D.M.; Doze, V.A. Cardiac and neuroprotection regulated by  $\alpha$ (1)-adrenergic receptor subtypes. *J. Recept. Signal Transduct. Res.* **2011**, *31*, 98–110. [[CrossRef](#)]
30. Shannon, R.; Chaudhry, M. Effect of alpha1-adrenergic receptors in cardiac pathophysiology. *Am. Heart J.* **2006**, *152*, 842–850. [[CrossRef](#)]
31. Anyukhovskiy, E.P.; Rosen, M.R. Abnormal automatic rhythms in ischemic Purkinje fibers are modulated by a specific alpha 1-adrenergic receptor subtype. *Circulation* **1991**, *83*, 2076–2082. [[CrossRef](#)]
32. Geller, J.C.; Cua, M.; Prieto, L.; Guo, S.D.; Danilo, P., Jr.; Rosen, M.R. Chloroethylclonidine increases the incidence of lethal arrhythmias during coronary occlusion in anesthetized dogs. *Eur. J. Pharmacol.* **1995**, *294*, 423–428. [[CrossRef](#)]
33. Yasutake, M.; Avkiran, M. Effects of selective alpha 1A-adrenoceptor antagonists on reperfusion arrhythmias in isolated rat hearts. *Mol. Cell. Biochem.* **1995**, *147*, 173–180. [[CrossRef](#)]
34. Suita, K.; Fujita, T.; Hasegawa, N.; Cai, W.; Jin, H.; Hidaka, Y.; Prajapati, R.; Umemura, M.; Yokoyama, U.; Sato, M.; et al. Norepinephrine-Induced Adrenergic Activation Strikingly Increased the Atrial Fibrillation Duration through  $\beta$ 1- and  $\alpha$ 1-Adrenergic Receptor-Mediated Signaling in Mice. *PLoS ONE* **2015**, *10*, e0133664. [[CrossRef](#)]
35. Luo, D.L.; Gao, J.; Fan, L.L.; Tang, Y.; Zhang, Y.Y.; Han, Q.D. Receptor subtype involved in alpha 1-adrenergic receptor-mediated  $\text{Ca}^{2+}$  signaling in cardiomyocytes. *Acta Pharmacol. Sin.* **2007**, *28*, 968–974. [[CrossRef](#)]
36. Yasutake, M.; Avkiran, M. Exacerbation of reperfusion arrhythmias by alpha 1 adrenergic stimulation: A potential role for receptor mediated activation of sarcolemmal sodium-hydrogen exchange. *Cardiovasc. Res.* **1995**, *29*, 222–230.
37. Desiniotis, A.; Kyprianou, N. Advances in the design and synthesis of prazosin derivatives over the last ten years. *Expert Opin. Ther. Targets* **2011**, *15*, 1405–1418. [[CrossRef](#)]
38. Li, H.; Xu, T.Y.; Li, Y.; Chia, Y.C.; Buranakitjaroen, P.; Cheng, H.M.; Van Huynh, M.; Sogunuru, G.P.; Tay, J.C.; Wang, T.D.; et al. Role of  $\alpha$ 1-blockers in the current management of hypertension. *J. Clin. Hypertens.* **2022**, *24*, 1180–1186. [[CrossRef](#)]
39. Marona, H.; Kubacka, M.; Filipek, B.; Siwek, A.; Dybała, M.; Szneler, E.; Pocięcha, T.; Gunia, A.; Waszkielewicz, A.M. Synthesis, alpha-adrenoceptors affinity and alpha 1-adrenoceptor antagonistic properties of some 1,4-substituted piperazine derivatives. *Pharmazie* **2011**, *66*, 733–739.
40. Wu, Y.; Zeng, L.; Zhao, S. Ligands of Adrenergic Receptors: A Structural Point of View. *Biomolecules* **2021**, *11*, 936. [[CrossRef](#)]

41. Handzlik, J.; Bajda, M.; Zygmunt, M.; Maciag, D.; Dybała, M.; Bednarski, M.; Filipek, B.; Malawska, B.; Kieć-Kononowicz, K. Antiarrhythmic properties of phenylpiperazine derivatives of phenytoin with  $\alpha_1$ -adrenoceptor affinities. *Bioorganic Med. Chem.* **2012**, *20*, 2290–2303. [[CrossRef](#)]
42. Waszkielewicz, A.M.; Kubacka, M.; Pańczyk, K.; Mogilski, S.; Siwek, A.; Głuch-Lutwin, M.; Gryboś, A.; Filipek, B. Synthesis and activity of newly designed aroxyalkyl or aroxyethoxyethyl derivatives of piperazine on the cardiovascular and the central nervous systems. *Bioorganic Med. Chem. Lett.* **2016**, *26*, 5315–5321. [[CrossRef](#)]
43. Bopp, C.; Auger, C.; Diemunsch, P.; Schini-Kerth, V. The effect of urapidil, an alpha-1 adrenoceptor antagonist and a 5-HT<sub>1A</sub> agonist, on the vascular tone of the porcine coronary and pulmonary arteries, the rat aorta and the human pulmonary artery. *Eur. J. Pharmacol.* **2016**, *779*, 53–58. [[CrossRef](#)]
44. Masumori, N. Naftopidil for the treatment of urinary symptoms in patients with benign prostatic hyperplasia. *Ther. Clin. Risk Manag.* **2011**, *7*, 227–238. [[CrossRef](#)]
45. Handzlik, J.; Maciag, D.; Kubacka, M.; Mogilski, S.; Filipek, B.; Stadnicka, K.; Kieć-Kononowicz, K. Synthesis, alpha 1-adrenoceptor antagonist activity, and SAR study of novel arylpiperazine derivatives of phenytoin. *Bioorganic Med. Chem.* **2008**, *16*, 5982–5998. [[CrossRef](#)]
46. Handzlik, J.; Pertz, H.H.; Görnemann, T.; Jähnichen, S.; Kieć-Kononowicz, K. Search for influence of spatial properties on affinity at  $\alpha_1$ -adrenoceptor subtypes for phenylpiperazine derivatives of phenytoin. *Bioorganic Med. Chem. Lett.* **2010**, *20*, 6152–6156. [[CrossRef](#)]
47. Handzlik, J.; Szymańska, E.; Wójcik, R.; Dela, A.; Jastrzębska-Więsek, M.; Karolak-Wojciechowska, J.; Fruziński, A.; Siwek, A.; Filipek, B.; Kieć-Kononowicz, K. Synthesis and SAR-study for novel arylpiperazine derivatives of 5-arylidenhydantoin with  $\alpha_1$ -adrenoceptor antagonistic properties. *Bioorganic Med. Chem.* **2012**, *20*, 4245–4257. [[CrossRef](#)]
48. Handzlik, J.; Bojarski, A.J.; Satała, G.; Kubacka, M.; Sadek, B.; Ashoor, A.; Siwek, A.; Więcek, M.; Kucwaj, K.; Filipek, B.; et al. SAR-studies on the importance of aromatic ring topologies in search for selective 5-HT<sub>7</sub> receptor ligands among phenylpiperazine hydantoin derivatives. *Eur. J. Med. Chem.* **2014**, *78*, 324–339. [[CrossRef](#)]
49. Barbaro, R.; Betti, L.; Botta, M.; Corelli, F.; Giannaccini, G.; Maccari, L.; Manetti, F.; Strappaghetti, G.; Corsano, S. Synthesis, biological evaluation, and pharmacophore generation of new pyridazinone derivatives with affinity toward alpha(1)- and alpha(2)-adrenoceptors. *J. Med. Chem.* **2001**, *44*, 2118–2132. [[CrossRef](#)]
50. Witek, K.; Latacz, G.; Kaczor, A.; Czekajewska, J.; Żesławska, E.; Chudzik, A.; Karczewska, E.; Nitek, W.; Kieć-Kononowicz, K.; Handzlik, J. Phenylpiperazine 5,5-Dimethylhydantoin Derivatives as First Synthetic Inhibitors of Msr(A) Efflux Pump in *Staphylococcus epidermidis*. *Molecules* **2020**, *25*, 3788. [[CrossRef](#)]
51. Groom, C.R.; Bruno, I.J.; Lightfoot, M.P.; Ward, S.C. The Cambridge Structural Database. *Acta Cryst. B* **2016**, *72*, 171–179. [[CrossRef](#)]
52. Foglar, R.; Shibata, K.; Horie, K.; Hirasawa, A.; Tsujimoto, G. Use of recombinant alpha 1-adrenoceptors to characterize subtype selectivity of drugs for the treatment of prostatic hypertrophy. *Eur. J. Pharmacol.* **1995**, *288*, 201–207. [[CrossRef](#)]
53. Takei, R.; Ikegaki, I.; Shibata, K.; Tsujimoto, G.; Asano, T. Naftopidil, a novel alpha1-adrenoceptor antagonist, displays selective inhibition of canine prostatic pressure and high affinity binding to cloned human alpha1-adrenoceptors. *Jpn. J. Pharmacol.* **1999**, *79*, 447–454.
54. Szkaradek, N.; Rapacz, A.; Pytka, K.; Filipek, B.; Siwek, A.; Cegła, M.; Marona, H. Synthesis and preliminary evaluation of pharmacological properties of some piperazine derivatives of xanthone. *Bioorganic Med. Chem.* **2013**, *21*, 514–522. [[CrossRef](#)]
55. Szkaradek, N.; Rapacz, A.; Pytka, K.; Filipek, B.; Żelaszczyk, D.; Szafranski, P.; Słoczyńska, K.; Marona, H. Cardiovascular activity of the chiral xanthone derivatives. *Bioorganic Med. Chem.* **2015**, *23*, 6714–6724. [[CrossRef](#)]
56. Manetti, F.; Corelli, F.; Strappaghetti, G.; Botta, M. Arylpiperazines with affinity toward alpha(1)-adrenergic receptors. *Curr. Med. Chem.* **2002**, *9*, 1303–1321. [[CrossRef](#)]
57. Betti, L.; Zanelli, M.; Giannaccini, G.; Manetti, F.; Schenone, S.; Strappaghetti, G. Synthesis of new piperazine-pyridazinone derivatives and their binding affinity toward alpha1-, alpha2-adrenergic and 5-HT<sub>1A</sub> serotonergic receptors. *Bioorganic Med. Chem.* **2006**, *14*, 2828–2836. [[CrossRef](#)]
58. Fukiyama, K.; Omae, T.; Iimura, O.; Yoshinaga, K.; Yagi, S.; Inagaki, Y.; Ishii, M.; Kaneko, Y.; Yamada, K.; Ijichi, H.; et al. A double-blind comparative study of doxazosin and prazosin in the treatment of essential hypertension. *Am. Heart J.* **1991**, *121 Pt 2*, 317–322. [[CrossRef](#)]
59. Joglekar, S.J.; Nanivadekar, A.S. A randomized, controlled, multicenter study to compare prazosin GITS with enalapril in hypertensive patients with diabetes mellitus. Bombay Hypertension Study Group. *J. Assoc. Physicians India* **1998**, *Suppl 1*, 52–62.
60. Burla, M.C.; Caliendo, R.; Carrozzini, B.; Cascarano, G.L.; Cuocci, C.; Ciazovazzo, C.; Mallamo, M.; Mazzone, A.G.; Polidori, G. Crystal structure determination and refinement via SIR2014. *J. Appl. Cryst.* **2015**, *48*, 306–309. [[CrossRef](#)]
61. Sheldrick, G.M. Crystal structure refinement with SHELXL. *Acta Cryst. C* **2015**, *71*, 3–8. [[CrossRef](#)]
62. Macrae, C.F.; Sovago, I.; Cottrell, S.J.; Galek, P.T.A.; McCabe, P.; Pidcock, E.; Platings, M.; Shields, G.P.; Stevens, J.S.; Towler, M.; et al. Mercury 4.0: From Visualization to Analysis, Design and Prediction. *J. Appl. Cryst.* **2020**, *53*, 226–235. [[CrossRef](#)]
63. Cheng, Y.; Prusoff, W.H. Relationship between the inhibition constant (K<sub>1</sub>) and the concentration of inhibitor which causes 50 per cent inhibition (I<sub>50</sub>) of an enzymatic reaction. *Biochem. Pharmacol.* **1973**, *22*, 3099–3108.
64. LigPrep. *Schrödinger Release 2019-4*; Schrödinger LLC: New York, NY, USA, 2019.
65. *Schrödinger Release 2019-4: Glide*; Schrödinger LLC: New York, NY, USA, 2019.

66. Pandey-Szekeres, G.; Munk, C.; Tsonkov, T.M.; Mordalski, S.; Harpsøe, K.; Hauser, A.S.; Bojarski, A.J.; Gloriam, D.E. GPCRdb in 2018: Adding GPCR structure models and ligands. *Nucleic Acids Res.* **2018**, *46*, D440–D446. [[CrossRef](#)]
67. Sali, A.; Blundell, T.L. Comparative protein modelling by satisfaction of spatial restraints. *J. Mol. Biol.* **1993**, *234*, 779–815. [[CrossRef](#)]
68. *The PyMOL Molecular Graphics System*, Version 2.3.2, Schrödinger LLC: New York, NY, USA, 2019.

**Disclaimer/Publisher’s Note:** The statements, opinions and data contained in all publications are solely those of the individual author(s) and contributor(s) and not of MDPI and/or the editor(s). MDPI and/or the editor(s) disclaim responsibility for any injury to people or property resulting from any ideas, methods, instructions or products referred to in the content.